Published in final edited form as:
Biochemistry. 2002 September 24; 41(38): 11411–11424.

C2 Domains of Protein Kinase C Isoforms α, β, and γ: Activation Parameters and Calcium Stoichiometries of the Membrane-Bound State†

Susy C. Kohout[‡], **Senena Corbalán-García**[§], **Alejandro Torrecillas**[§], **Juan C. Goméz-Fernandéz**[§], and **Joseph J. Falke**[*,‡]

[‡]Department of Chemistry and Biochemistry, UniVersity of Colorado, Boulder, Colorado 80309-0215

[§]Departamento de Bioquimica y Biologia Molecular (A), Facultad de Veterinaria, Universidad de Murcia, Apartado de Correos 4021, E30080 Murcia, Spain

Abstract

The independently folding C2 domain motif serves as a Ca^{2+}-dependent membrane docking trigger in a large number of Ca^{2+} signaling pathways. A comparison was initiated between three closely related C2 domains from the conventional protein kinase C subfamily (cPKC, isoforms α, β, and γ). The results reveal that these C2 domain isoforms exhibit some similarities but are specialized in important ways, including different Ca^{2+} stoichiometries. In the absence of membranes, Ca^{2+} affinities of the isolated C2 domains are similar (2-fold difference) while Hill coefficients reveal cooperative Ca^{2+} binding for the PKCβ C2 domain but not for the PKCα or PKCγ C2 domain (H = 2.3 ± 0.1 for PKCβ, 0.9 ± 0.1 for PKCα, and 0.9 ± 0.1 for PKCγ). When phosphatidylserine-containing membranes are present, Ca^{2+} affinities range from the sub-micromolar to the micromolar (7-fold difference) ($[Ca^{2+}]_{1/2}$ = 0.7 ± 0.1 μM for PKCγ, 1.4 ± 0.1 μM for PKCα, and 5.0 ± 0.2 μM for PKCβ), and cooperative Ca^{2+} binding is observed for all three C2 domains (Hill coefficients equal 1.8 ± 0.1 for PKCβ, 1.3 ± 0.1 for PKCα, and 1.4 ± 0.1 for PKCγ). The large effects of membranes are consistent with a coupled Ca^{2+} and membrane binding equilibrium, and with a direct role of the phospholipid in stabilizing bound Ca^{2+}. The net negative charge of the phospholipid is more important to membrane affinity than its headgroup structure, although a slight preference for phosphatidylserine is observed over other anionic phospholipids. The Ca^{2+} stoichiometries of the membrane-bound C2 domains are detectably different. PKCβ and PKCγ each bind three Ca^{2+} ions in the membrane-associated state; membrane-bound PKCα binds two Ca^{2+} ions, and a third binds weakly or not at all under physiological conditions. Overall, the results indicate that conventional PKC C2 domains first bind a subset of the final Ca^{2+} ions in solution, and then associate weakly with the membrane and bind additional Ca^{2+} ions to yield a stronger membrane interaction in the fully assembled tertiary complex. The full complement of Ca^{2+} ions is needed for tight binding to the membrane. Thus, even though the three C2 domains are 64% identical, differences in Ca^{2+} affinity, stoichiometry, and cooperativity are observed, demonstrating that these closely related C2 domains are specialized for their individual functions and contexts.

†Support provided by NIH Grants GM R01-63235 (to J.J.F.) and GM T32-07135 (to S.C.K.) and by DGESIC Grant PB98-0389 (to J.C.G.-F.).

*To whom correspondence should be addressed. falke@colorado.edu. Telephone: (303) 492-3503. Fax: (303) 492-5894.

Calcium is a ubiquitous second messenger in eukaryotic cells which regulates a wide variety of signaling pathways such as fertilization, gene transcription, cell division, differentiation, muscle contraction, neuronal signaling, inflammation, and programmed cell death (1, 2). The Ca^{2+} transients responsible for transmitting information are precisely regulated in space, time, and concentration (1). Together, these variables are optimized to create distinct Ca^{2+} signals which can coexist even in the same cell type, yet are highly specialized for activation of different pathways. It follows that the cytoplasmic proteins responsible for detecting, interpreting, and propagating these Ca^{2+} signals should be equally specialized. In particular, the Ca^{2+} binding and activation parameters of a given protein should be "tuned" to match the spatial and temporal properties of the appropriate Ca^{2+} transient (3, 4).

The conserved C2 domain is a Ca^{2+}-activated membrane targeting motif present in a wide range of Ca^{2+}-regulated proteins (5, 6). Prototypical C2 domains bind multiple Ca^{2+} ions and then dock to specific intracellular membranes, thereby allowing their associated domains to regulate an important membrane signaling event (7). There are at least five intracellular protein families which contain C2 domains: (i) protein kinases that phosphorylate membrane-associated targets, (ii) phospholipid-modifying enzymes that activate or inactivate lipid-derived second messengers, (iii) vesicle targeting and fusion proteins, (iv) GTPase-activating proteins, and (v) ubiquitination enzymes that target membrane proteins for degradation (5, 6). There are several C2 domains of known structure, including those from cytosolic phospholipase A2 (8–10), synaptotagmin (11–13), phospholipase Cδ (14, 15), protein kinase CβI (16), protein kinase Cα (17), protein kinase Cδ (18), protein kinase Cε (19), PTEN (20), and PI3K (21). They all share a canonical β sandwich structure composed of two, four-stranded anti-parallel β sheets, and the three interstrand loops generally implicated in Ca^{2+} binding lie at one end of the motif. The known tertiary structures are remarkably similar given the low level of sequence similarity seen between C2 domains (5). The primary structures and lengths of the Ca^{2+} binding loops, as well as the number of Ca^{2+} binding sites, vary from protein to protein as would be expected for related domains specialized for different signaling applications. Previous work has already characterized the dramatic specialization of C2 domains from different functional families (4).

To elucidate the features of the C2 domain that are specialized within a single functional family, a comparison of C2 domains from the same family, known to share similar primary and tertiary structures, would be useful. There are three subfamilies and at least 10 isoforms of PKC. The conventional protein kinase C (cPKC)[1] subfamily includes isoforms α, β, and γ, which are suitable candidates for a comparison of functionally homologous C2 domains. In vitro, the α, β, and γ isoforms of cPKC phosphorylate the same natural target peptides to a similar degree (22); however, the accumulating in vivo evidence indicates a larger degree of functional specialization (for a review of PKC regulation, see ref 23). The normal expression levels of cPKCs give some indication of specialization since PKCα is found in all cell types, PKCβ is found in a subset of cell types, and PKCγ is found only in the brain (24). Overexpression of PKCα is believed to contribute to the transformation and proliferation of malignancies, while PKCβ is used as a marker for certain types of cancer, and its overexpression has been implicated in heart failure and diabetic cardiovascular complications (25–28). Moreover, PKCγ has been implicated in the development of injury-induced persistent pain (29, 30). (for a review of the different roles of PKC isoforms in cancers, see ref 31). Another indication that in vivo specialization exists for these isoforms

[1]Abbreviations: PKC, protein kinase C; PC, phosphatidylcholine; PS, phosphatidylserine; dPE, *N*-[5-(dimethylamino)naphthalene-1-sulfonyl]-1,2-dihexadecanoyl-*sn*-glycero-3-phosphoethanolamine; GST, glutathione S-tranferase; FRET, fluorescence resonance energy transfer; DTT, dithiothreitol; HEPES, *N*-(2-hydroxyethyl)piperazine-*N*′-2-ethanesulfonic acid; EDTA, ethylenediaminetetraacetic acid.

comes from a study which determined that the primary cPKC isoform activated by angiotensin II changed among α, β, and γ depending of the age of the rat (32). Some degree of specialization may come from protein interactions between PKCs and receptor-activated C kinases or RACKs (33). Two RACKs have been identified thus far, RACK 1 and β′-COP (34, 35), which have been found to bind to PKCβ and PKCε, respectively. A binding site for RACKs on PKCβ has been localized to Ca^{2+} binding loops 1 and 2 and strand 4 using peptides based on those regions (36). The V5 region has also been implicated in binding to RACKs (37).

The C2 domains of cPKC isoforms α, β, and γ are 64% identical in their primary amino acid sequences (Figure 1) (38–40). Moreover, the known crystal structures of the PKCα and PKCβ C2 domains exhibit an only 0.43 Å rms deviation between the equivalent C_α atoms (Figure 2) (16, 17). Interestingly, the PKCα C2 domain has been cocrystallized with two different short chain phosphatidylserine (PS) lipid analogues (17, 41), revealing that lipid oxygens directly coordinate one or more of the bound Ca^{2+} ions and thus can play an important role in Ca^{2+} binding. It is notable that the available structures exhibit variability in the number of bound Ca^{2+} ions, ranging from two to three for PKCα and three for PKCβ, and that the relevant Ca^{2+} stoichiometry for PKC C2 domain docking to membranes remains unclear (16, 17, 41). Moreover, specific interactions between bound Ca^{2+} ions and lipid headgroups on the membrane surface are supplemented by nonspecific electrostatic interactions that help stabilize the membrane-docked state of the protein–Ca^{2+} complex (42). Although no structural information is available for PKCγ, the high level of sequence identity indicates that the PKCγ C2 domain possesses a structure similar to that of C2 domains from other conventional PKCs. In particular, the PKCγ C2 domain is 73 and 67% identical to the PKCα and PKCβ C2 domains, respectively (38–40).

In the study presented here, a comparison was initiated between the C2 domains of conventional PKC isoforms α, β, and γ to determine if these closely related C2 domains exhibit functional specializations, and to determine their Ca^{2+} stoichiometries in the membrane-docked state. Using steady state fluorescence, fluorescence resonance energy transfer (FRET), and stopped flow methods, the equilibrium and kinetic features of Ca^{2+} and membrane binding were analyzed for each isolated domain. The results demonstrate that even closely related C2 domains can exhibit specialized Ca^{2+} activation parameters.

MATERIALS AND METHODS

Reagents

The lipids that were used were 1-palmitoyl-2-oleoyl-*sn*-glycero-3-phosphocholine (phosphatidylcholine, PC), 1-palmitoyl-2-oleoyl-*sn*-glycero-3-phosphoserine (phosphatidylserine, PS), 1-palmitoyl-2-oleoyl-*sn*-glycero-3-phosphoglycerol (phosphatidylglycerol, PG), 1-palmitoyl-2-oleoyl-*sn*-glycero-3-phosphoinositol (phosphatidylinositol, PI), and 1-palmitoyl-2-oleoyl-*sn*-glycero-3-phosphoethanolamine (phosphatidylethanolamine, PE), all from Avanti Polar Lipids. Magnesium green, Quin-2, and *N*-[5-(dimethylamino)naphthalene-1-sulfonyl]-1,2-dihexadecanoyl-*sn*-glycero-3-phosphoethanolamine (dansyl-PE or dPE) were from Molecular Probes. Small unilamellar phospholipid vesicles were prepared by sonication. Solutions and plasticware were decalcified as described previously (43).

Purification of C2 Domains

The C2 domain of PKCβ was expressed as a glutathione *S*-transferase (GST) fusion protein and isolated on a glutathione affinity column prior to cleavage with thrombin and elution of the free C2 domain (16). The C2 domains of PKCα and PKCγ were expressed with a His

tag and isolated using a nickel affinity column prior to cleavage with thrombin and removal of the free His tag via a second nickel column (17). Protein concentrations were determined by tryptophan absorbance, the BCA assay, and SDS–PAGE gels (44–46).

Equilibrium Fluorescence Experiments

Equilibrium fluorescence experiments were carried out on an SLM 48000S fluorescence spectrometer at 25 °C in standard assay buffer composed of 20 mM *N*-(2-hydroxyethyl)piperazine-*N*′-2-ethanesulfonic acid (HEPES) (pH 7.4) with KOH, 100 mM KCl, and 5 mM dithiothreitol (DTT). The excitation and emission slit widths were 4 and 8 nm, respectively, for all equilibrium fluorescence experiments.

To determine domain stability, C2 domain (0.5 μM) in the absence of vesicles and calcium was titrated with a concentrated stock of urea in standard assay buffer. The intrinsic tryptophan fluorescence was monitored using excitation (λ_{ex}) and emission (λ_{em}) wavelengths of 284 and 340 nm, respectively. Data were fit with the following equation:

$$\Delta F = \frac{F_N + F_D K_o e^{-cx}}{1 + K_o e^{-cx}} \quad (1)$$

where F_N represents the fluorescence of the native protein, F_D represents the fluorescence of the denatured protein, K_o represents the equilibrium constant for unfolding extrapolated to zero urea, c represents a proportionality constant, and x is the urea concentration (47). The free energy of unfolding in the absence of urea was then calculated as $\Delta G_D^{H_2O} = -RT \ln K_o$.

To monitor Ca^{2+} binding to the free C2 domain, a concentrated Ca^{2+} stock in standard buffer was titrated into a sample containing the C2 domain (0.5 μM) in standard buffer lacking vesicles. The intrinsic tryptophan fluorescence was monitored using the same excitation and emission wavelengths indicated above. To control for tryptophan quenching, a separate cuvette with the C2 domain alone was monitored. The control was subtracted from the Ca^{2+} titration data following correction for dilution. The maximum fluorescence was normalized to 1.

To monitor the Ca^{2+} dependence of C2 domain docking to membrane, tryptophan quenching due to protein-to-membrane fluorescence resonance energy transfer (FRET) was monitored in the presence of a fluorescent chelator, magnesium green (MAG), which quantitated the free Ca^{2+} concentration. Details of this method have been previously described (48–50). C2 domain (0.5 μM) in standard buffer was titrated with a concentrated Ca^{2+} stock in standard buffer in the presence of PC, PS, and dPE (47.5%:47.5%:5% mole percent, 250 μM total phospholipid) and MAG (0.5 μM). Trp quenching was monitored using excitation (λ_{ex}) and emission (λ_{em}) wavelengths of 284 and 340 nm, respectively. Free Ca^{2+} was monitored via the MAG fluorescence generated by excitation (λ_{ex}) and emission (λ_{em}) wavelengths of 506 and 532 nm, respectively. The K_D for Ca^{2+} binding to MAG was determined experimentally by titrating MAG in standard buffer with Ca^{2+}, enabling quantitation of free Ca^{2+} in the protein sample using the following equation:

$$[Ca^{2+}]_{free} = K_D \left(\frac{F - F_{min}}{F_{max} - F} \right) \quad (2)$$

where F is the fluorescence at a given Ca^{2+} concentration, F_{min} is the minimum fluorescence observed in the titration, and F_{max} is the maximum fluorescence observed in the titration (50).

Phospholipid headgroup specificity experiments were carried out by titrating each C2 domain with vesicles composed of PC, PX, and dPE (72.5%:22.5%:5% mole percent), where PX was PS, PG, PI, or PE. The titrations were first carried out using PC and dPE (95%:5% mole percent), and no appreciable binding was observed. C2 domain (0.5 μM) was premixed with 1 mM EDTA and 2 mM Ca^{2+} (net 1 mM free Ca^{2+}) in standard assay buffer. Sonicated lipids were titrated in, and the protein-to-membrane FRET was monitored from the dPE emission using excitation (λ_{ex}) and emission (λ_{em}) wavelengths of 284 and 520 nm, respectively. The titration of phospholipid into buffer lacking protein was used to control for the increasing background emission arising from direct dPE excitation. For each C2 domain, the affinity for a standard mixture of PC, PS, and dPE (47.5%:47.5%:5% mole percent) was also determined using the same conditions described above, to enable direct comparisons with the other equilibrium and kinetic parameters determined using this standard lipid mixture. All total lipid concentrations in lipid affinity measurements are divided by 2 to take into account the inaccessibility of one leaflet to protein, due to the sealed nature of the bilamellar sonicated vesicles.

The dependence of protein docking on PS density was determined by varying the mole percent of PS in a mixture with PC and dPE. The following mole percents were used: 95%: 5% PS/dPE, 76%:19%:5% PS/PC/dPE, 57%:38%:5% PS/PC/dPE, 38%:57%:5% PS/PC/ dPE, 28.5%:66.5%:5% PS/PC/dPE, 19%:76%:5% PS/PC/dPE, and 9.5%:85.5%:5% PS/PC/ dPE mixtures. Protein-to-membrane FRET was monitored via dPE emission using the same conditions described above. All total lipid concentrations were divided by 2 to take into account the inaccessibility of one leaflet to protein.

All equilibrium binding data were subjected to a nonlinear, least-squares analysis using either the single-independent site equation (eq 3) or the Hill equation (eq 4). In particular, all lipid titrations were analyzed by the single-independent site equation (eq 3), while Ca^{2+} titrations often exhibited positive cooperativity and thus were analyzed by the Hill equation (eq 4):

$$\Delta F = \Delta F_{max}\left(\frac{x}{K_D + x}\right) \quad (3)$$

$$\Delta F = \Delta F_{max}\left(\frac{x^H}{[Ca^{2+}]_{1/2}{}^H + x^H}\right) \quad (4)$$

where ΔF_{max} represents the calculated maximal fluorescence change, x represents either the free Ca^{2+} concentration (for Ca^{2+} titrations) or the phospholipid concentration corrected for the leaflet effect (for phospholipid titrations), K_D represents the macroscopic equilibrium dissociation constant for lipid binding, and $[Ca^{2+}]_{1/2}$ represents the Ca^{2+} concentration that yields half-maximal binding. Nonlinear least-squares analysis was used to determine the best fit of each equation to the experimental data, yielding the apparent K_D or $[Ca^{2+}]_{1/2}$ and, in the case of eq 4, the Hill coefficient (H).

To estimate the number of PS molecules interacting with each membrane-bound C2 domain, protein was titrated into vesicle samples containing 1 mM free Ca^{2+} in standard buffer. The lipid mixtures that were chosen utilized a low PS mole percent to minimize protein crowding, but the vesicle concentration was high enough to ensure that approximately 80% of the protein that was added was bound to the membrane. Protein was added until the maximal protein-to-membrane FRET signal was achieved, indicating saturation of the available lipid binding sites. Two different PC/PS/dPE mixtures were used to ensure the reproducibility of the data and to control for any protein crowding on the vesicle surface:

73.5%:22.5%:5% at 200 μM total lipid and 83.5%:11.5%:5% at 380 μM total lipid. For the data analysis, the total PS concentration was divided by 2 to take into account the inaccessibility of one leaflet, yielding the accessible PS concentration. The total concentration of protein was then divided by the available PS concentration to yield the protein:PS mole ratio. The protein-to-membrane FRET signal was plotted against this ratio, and the minimal ratio at which the FRET signal reached a plateau was determined. To estimate the number of PS molecules per C2 domain, the reciprocal of the plateau protein:PS ratio was calculated.

The effect of ionic strength on protein docking to the membrane was tested by titrating NaCl into samples containing the ternary complex of the C2 domain (0.5 μM), Ca^{2+} (1 mM free), and vesicles (250 μM total PC, PS, and dPE, 47.5%:47.5%:5% mole percent). The buffer that was used was standard buffer lacking KCl. The decreasing FRET signal was monitored. The contribution of the hydrophobic effect to docking was analyzed using the chaotropic salt Na_2SO_4, which enhances the hydrophobic effect (51, 52). Na_2SO_4 was titrated into a mixture of the apo-C2 domain and vesicles (PC/PS/dPE, 47.5%:47.5%:5% mole percent) in standard buffer in the absence of free Ca^{2+}, and membrane docking was monitored by protein-to-membrane FRET. As a positive control, the isolated C2 domain of cytosolic phospholipase A2 was monitored; this domain utilizes a hydrophobic docking mechanism and is stimulated by Na_2SO_4 to bind to vesicles in the absence of Ca^{2+} (51).

Kinetic Fluorescence Experiments

All kinetic experiments were carried out on an Applied Photophysics SX.17 stopped flow fluorescence instrument at 25 °C in standard buffer unless otherwise noted. The dead time of the instrument was 0.9 ± 0.1 ms; thus, all data before 1 ms were removed prior to analysis. The slit width on the excitation monochromator was 3 nm for all kinetic experiments, while filters were used to select the detected wavelengths of emitted light.

To determine the rate constant of membrane docking, two different experiments were performed. First, the C2 domain (1 μM) was premixed with saturating Ca^{2+} (1 mM free) and then rapidly mixed with vesicles (500 μM total PC, PS, and dPE, 47.5%:47.5%:5% mole percent). The development of protein-to-membrane FRET was observed by exciting the sample with a λ_{ex} of 284 nm light while monitoring dPE emission using a 475 nm long pass filter. The resulting time course was fit with a single-exponential equation (4). In the second experiment, the Ca^{2+} and vesicles were premixed, and then the reaction was started by mixing with the C2 domain (all concentrations as for the first experiment).

To determine the rate constant for dissociation of the C2 domain from the membrane following removal of free Ca^{2+}, the experiment began with the preformed ternary complex of the C2 domain (1 μM), Ca^{2+} (1 mM free), and PC/PS/dPE vesicles (47.5%:47.5%:5% mole percent) in standard buffer. At time zero, the ternary complex was rapidly mixed with 10 mM EDTA to chelate all free Ca^{2+}. As a result, the membrane dissociation reaction became irreversible since there was no free Ca^{2+} to drive redocking to the membrane. The resulting decrease in the protein-to-membrane FRET signal, measured as described above for the kinetic analysis of membrane association, was fit with a single-exponential equation.

To determine the Ca^{2+} stoichiometry and Ca^{2+} dissociation rate constant of the membrane-bound ternary complex, the fluorescent Ca^{2+} chelator Quin-2 was used. This chelator was used to count the number of free Ca^{2+} ions released from the protein into solution by using excess chelator at Ca^{2+} concentrations well over the K_D for Ca^{2+} binding to Quin-2. Details of the method have been previously described (4, 53, 54). The preformed ternary complex [2 μM C2 domain, 100 μM Ca^{2+}, and 500 μM PC and PS (50%:50% mole percent)] was rapidly mixed with excess Quin-2 (200 μM), while Quin-2 fluorescence was excited at a λ_{ex}

of 335 nm and monitored with a 475 nm long pass filter. The resulting Ca^{2+}-Quin-2 fluorescence increase was fit with a single-exponential equation. In a parallel experiment, a standard curve was constructed by mixing a range of free Ca^{2+} concentrations (60–140 μM) with Quin-2 (200 μM) and then plotting the resulting fluorescence changes from baseline (0 μM Ca^{2+}) versus the concentration of free Ca^{2+}. The slope of the best fit straight line represents the fluorescence change per micromolar Ca^{2+} released. Finally, the fluorescence change observed for Ca^{2+} release from the ternary complex was interpolated on this standard curve to determine the concentration of released Ca^{2+}, and then compared to the concentration of the C2 domain to calculate the Ca^{2+} stoichiometry of the ternary complex.

RESULTS

Preparation and Stabilities of the Isolated PKCα, PKCβI, and PKCγ C2 Domains

The isolated C2 domains from PKCα, PKCβI, and PKCγ were expressed in *Escherichia coli* and purified to homogeneity. The affinity tags used to purify the C2 domains (His tag for PKCα and PKCγ and GST fusion for PKCβ) were removed via thrombin cleavage, followed by an additional chromatography step to remove the free affinity tag and protease. The buffer used for C2 domain storage, unless otherwise specified, was 20 mM HEPES (pH 7.4), 100 mM KCl, and 5 mM DTT, and all experiments were conducted at 25 °C.

The stability of the isolated C2 domains toward unfolding by a chemical denaturant was examined to confirm that each domain was folded, and to compare their relative intrinsic stabilities in the absence of Ca^{2+} and membranes. Unfolding was detected utilizing the decrease in intrinsic tryptophan fluorescence that occurred as urea was titrated into a sample of each domain, as illustrated in Figure 3. The data were best fit with a two-state unfolding model (eq 1 in Materials and Methods), allowing determination of the equilibrium constant for unfolding at zero urea (47). In turn, this equilibrium constant was converted to the free energy of unfolding at zero urea as summarized in Table 1. All three domains were stably folded, exhibiting a cooperative urea denaturation profile. The PKCγ C2 domain is the most stable of the three C2 domains, yielding a free energy of unfolding that is 10 kJ/mol higher than that of the PKCα C2 domain, which was the least stable. Since the primary sequences of the three C2 domains are 62% identical, the contrasting stabilities must arise from a limited group of unconserved residues.

Calcium Binding to the Free C2 Domains in the Absence of Membranes

To determine the Ca^{2+} binding affinities of the three C2 domains in the absence of membranes, their intrinsic tryptophan fluorescences were tested and found to undergo emission changes upon Ca^{2+} binding. Each C2 domain was titrated with Ca^{2+}, and the resulting fluorescence curves were subjected to best fitting with both the single-independent site model and the Hill multisite model. The model which provided the superior fit was determined by χ^2 (Figure 4A). The data for PKCα were fitted best by the single-independent site model with an observed $[Ca^{2+}]_{1/2}$ of 35 ± 4 μM, indicating that this Ca^{2+} binding event is not cooperative. When fitted with the Hill model, the $[Ca^{2+}]_{1/2}$ was unchanged and the Hill coefficient was 0.9 ± 0.1, again indicating a lack of cooperativity. The data for PKCβ were fitted best by the Hill model with an observed $[Ca^{2+}]_{1/2}$ of 42 ± 2 μM and a Hill coefficient of 2.3 ± 0.1. The results for PKCγ were similar to those for PKCα in that no cooperativity was observed, while the $[Ca^{2+}]_{1/2}$ was lowered to 18 ± 2 μM. The lack of cooperativity for the free PKCα and PKCγ C2 domains suggests that Ca^{2+} binding to these domains is dominated by a single, independent Ca^{2+} ion, while the free PKCβ C2 domain binds multiple Ca^{2+} ions with positive cooperativity. Interestingly, although the three domains possess the same four tryptophans at identical positions (Figure 1), Ca^{2+} binding decreases the fluorescence of the PKCα and PKCγ C2 domains but increases the

fluorescence of the PKCβ C2 domain (Figure 4A). This finding is correlated with the number of Ca^{2+} ions bound to the free domain, indicating that the binding of a single Ca^{2+} ion to PKCα and PKCγ C2 domains generates a different tryptophan environmental change than the binding of multiple Ca^{2+} ions to the PKCβ C2 domain.

Calcium Binding to the Free C2 Domains in the Presence of Membranes

The Ca^{2+} binding affinity in the presence of membranes was measured by quantitating FRET between intrinsic tryptophan donors in the C2 domain and acceptor dansyl fluorophores in synthetic membrane vesicles. The vesicles contained an equimolar mixture of phosphatidylcholine (PC) and phosphatidylserine (PS), as well as a small mole ratio (5%) of dansyl-labeled phosphatidylethanolamine (dPE). The FRET signal monitors the membrane docking event, so the observed signal comes from C2 domains interacting with the membrane. No FRET signal was detected in the absence of Ca^{2+}, indicating that the apo domains have little or no membrane affinity prior to Ca^{2+} binding. Magnesium green, a fluorescent indicator for divalent cations, was included in the samples being titrated with Ca^{2+} to monitor the free Ca^{2+} concentration. The resulting protein-to-membrane FRET data were plotted against the free Ca^{2+} concentration and fitted best with the Hill model as illustrated in Figure 4B. The best-fit $[Ca^{2+}]_{1/2}$ values that yield the half-maximal FRET signal are 1.4 ± 0.1 μM for PKCα, 5.0 ± 0.2 μM for PKCβ, and 0.7 ± 0.1 μM for PKCγ. Thus, PKCγ exhibits the highest Ca^{2+} affinity in the membrane docking reaction, while PKCβ exhibits the lowest Ca^{2+} affinity. The best-fit Hill coefficients [1.3 ± 0.1 for PKCα, 1.8 ± 0.1 for PKCβ, and 1.4 ± 0.1 for PKCγ (Table 1)] indicate that membrane docking is driven by the binding of multiple Ca^{2+} ions with positive cooperativity for each domain. Clearly, the membrane has a significant effect on the Ca^{2+} binding of PKC C2 domains, particularly the PKCα and PKCγ C2 domains for which no positive cooperativity was observed in the absence of membranes.

Lipid Specificities of the C2 Domains

The lipid specificities of the three C2 domains were determined by monitoring the protein-to-membrane FRET signal when lipids possessing different headgroups were titrated into a solution of the C2 domain and saturating Ca^{2+}. Five different lipid headgroups were tested, including three anionic headgroups (PS, PG, and PI) and two neutral/zwitterionic headgroups (PC and PE). All lipids were tested as a mixture with PC at a PC:PX mole ratio of 3:1 with a small amount (5 mol %) of the dansylated lipid dPE. As shown in Figure 5A–C, the anionic headgroups induced protein docking while the zwitterionic headgroups did not. Since vesicles containing only PC and dPE failed to trigger detectable docking, the mixtures containing another lipid should accurately reflect the effect of the latter headgroup. Vesicles containing PS exhibited 2–5-fold higher C2 domain binding affinities than those containing other anionic phospholipids (see the legend of Figure 5A–C), which is consistent with the known biological importance of PS in activating full-length cPKCs (23). To directly compare the lipid affinities of the three C2 domains, their binding to mixed PC/PS/dPE vesicles was assessed in side-by-side protein-to-membrane FRET experiments as illustrated in Figure 5D. The resulting lipid dependences of protein docking are similar for all three C2 domains, yielding apparent K_Ds for PS binding in the 3–5 μM range as summarized in Table 1. Overall, the lipid specificity measurements indicate that membrane docking requires a phospholipid possessing a net negative charge, and that this charge is more important than the detailed structure of the headgroup. However, the C2 domain does possess a weak, specific interaction with the PS headgroup in the protein–membrane complex since the affinity of each C2 domain for this phospholipid is slightly higher than for PI and PG despite their equivalent net negative charges. Thus, the C2 domain contributes to the PS selectivity of conventional PKC isoforms, thereby supplementing the known interaction of the C1 domain with PS (55).

The dependence of protein docking on the concentration of PS in the vesicle mixtures was tested by changing the total mole ratio of PS in mixtures with PC and dPE. The mole ratio of PS was varied from 9.5 to 95%; dPE was held constant at 5%, and PC comprised the remaining percentage. The lipid titration was repeated for each new mole ratio of PS and the FRET signal recorded. The resulting binding curves were fitted best to an independent site model, yielding an apparent K_D for PS. Above 40% PS, the apparent K_Ds stabilize around 2–3 μM. Below 40% PS, however, the apparent K_Ds increase to at least 7 μM as the PS mole ratio decreases. Figure 6 plots the apparent K_Ds against the mole fraction of PS, revealing the similar behaviors of the three C2 domains in this experiment. The results raise the possibility that different intracellular membranes containing contrasting PS mole ratios could exhibit significantly different affinities for C2 domains, thereby affecting cellular targeting of cPKCs.

Lipid Stoichiometries of the C2 Domains

To further probe C2 domain binding to membranes, the lipid stoichiometry of the interaction was determined. Protein-to-membrane FRET was monitored for a suspension of vesicles and Ca^{2+} while titrating in a given C2 domain. At low protein concentrations, the FRET signal increased linearly with protein addition, while at high protein concentrations, the FRET signal stabilized at a constant plateau, indicating that the membrane binding sites had become saturated with protein (data not shown). The intersection of the linear rise and the flat plateau was determined by best-fit analysis, directly revealing the number of protein molecules bound per PS molecule. As shown in Table 1, the stoichiometry is 3 ± 1 PS headgroups per protein for PKCα, 4 ± 1 PS headgroups per protein for PKCβ, and 5 ± 1 PS headgroups per protein for PKCγ. These measured lipid stoichiometries, ranging from 3 to 5 PS headgroups per C2 domain, are within experimental error of one another, suggesting that the headgroup interactions and membrane footprints of the three domains are similar.

Ionic Nature of the Membrane Interaction

Previous studies have indicated that the binding of the PKCβ C2 domain or the synaptotagmin I C2A domain to PS-containing membranes is largely ionic, while the binding of the cytosolic phospholipase A2 C2 domain to membranes is primarily hydrophobic (4). To directly compare the forces underlying the membrane docking of the PKCα, PKCβ, and PKCγ C2 domains, two experiments were conducted. First, NaCl was added to a preformed ternary complex of Ca^{2+}, the C2 domain, and mixed PC/PS/dPE vesicles. Protein-to-membrane FRET measurements revealed that addition of NaCl caused dissociation of the PKCα and PKCγ C2 domains from the membrane, as previously observed for the PKCβ C2 domain, while the cytosolic phospholipase A2 C2 domain was unaffected (Figure 7A). Thus, the docking of all three cPKC C2 domains to PS-containing membranes requires electrostatic interactions that can be disrupted by high salt concentrations. The second experiment tested the ability of sodium sulfate, known to strengthen hydrophobic interactions (51, 52), to drive membrane docking in the absence of Ca^{2+}. In this experiment, sodium sulfate failed to trigger protein-to-membrane FRET for the PKCα and PKCγ C2 domains, as previously observed for the PKCβ C2 domain, while the cytosolic phospholipase A2 C2 domain showed a dramatic increase in the level of protein docking (Figure 7B). Thus, in contrast to the primarily hydrophobic docking mechanism of the cytosolic phospholipase A2 C2 domain, the cPKC C2 domains exhibit predominantly electrostatic interactions with membranes. These findings help explain the selectivity of the cPKC C2 domains for anionic lipid headgroups.

Kinetics of the C2 Domain Binding Events

To compare the kinetics of ligand binding and dissociation for the three C2 domains, stopped flow fluorescence methods were utilized to monitor the time courses of Ca^{2+} and

membrane binding and dissociation events. The Ca^{2+} binding equilibrium of the free C2 domains was found to be too fast to monitor by stopped flow methods; however, the docking of the Ca^{2+}-loaded domain to membranes and the dissociation of protein and Ca^{2+} from the membrane-bound complex were slow enough to be analyzed.

The kinetics of Ca^{2+}-triggered membrane docking were examined using the protein-to-membrane FRET assay to monitor docking. This docking reaction involves two types of events: the binding of multiple Ca^{2+} ions and protein docking to the membrane. To determine whether Ca^{2+} or membrane binding is rate-limiting, the stopped flow reaction was carried out with two alternate mixing schemes. In one, the C2 domain is pre-equilibrated with saturating Ca^{2+} before rapid mixing with membranes, yielding the time course of membrane docking for the Ca^{2+}-loaded protein. In the other, the free C2 domain is mixed with a suspension of Ca^{2+} and membranes such that Ca^{2+} binding to the protein must occur before the membrane docking reaction can proceed. Panels A–C of Figure 8 illustrate the two resulting time courses for each C2 domain. For each C2 domain, the two mixing protocols yield nearly identical time courses of protein-to-membrane FRET, indicating that the membrane docking reaction is strongly rate-limiting. Additional evidence supporting this conclusion is provided by the strong dependence of the FRET time course on the vesicle concentration (compare panels A–C with panel D of Figure 8, the latter obtained for a higher vesicle concentration). Interestingly, for PKCβ and PKCγ, membrane docking is delayed slightly when the protein is not pre-equilibrated with Ca^{2+}, indicating that a fast Ca^{2+} binding or protein conformational event occurs in the free protein before slower membrane docking, and that this rapid predocking event is complete within 2 ms. Direct comparison of the membrane docking time courses for the three Ca^{2+}-loaded C2 domains reveals their striking similarity, as illustrated in Figure 8D. Thus, under the conditions utilized in this study, the membrane association event is rate-limiting in the Ca^{2+}-triggered docking reactions of all three C2 domains.

The kinetics of dissociation of the C2 domain from the ternary complex of protein, Ca^{2+}, and vesicles were determined by mixing the preformed ternary complex with EDTA to chelate the Ca^{2+} ions as the complex dissociated, thereby making the dissociation reaction essentially irreversible. The resulting loss of protein-to-membrane FRET as the complex dissociates is observed in Figure 8E, wherein the dissociation kinetics of the C2 domains differ by more than 3-fold. PKCα dissociates most slowly with a rate constant of 17.3 ± 0.7 s^{-1}, while PKCγ is intermediate at 22 ± 1 s^{-1} and PKCβ fastest at 57 ± 7 s^{-1} [within error of the previously determined value for PKCβ (4); see Table 2]. Thus, the three C2 domains exhibit different membrane-bound state lifetimes ranging from 17 to 58 ms, with PKCα exhibiting the longest-lived ternary complex.

The kinetics of dissociation of Ca^{2+} from the ternary complex were determined by mixing the preformed complex with Quin-2, a fluorescent Ca^{2+} chelator. This experiment also revealed the stoichiometry of Ca^{2+} binding in the ternary complex. Quin-2 has a very high Ca^{2+} affinity and binds all the free Ca^{2+} within the dead time of the stopped flow instrument. Figure 9 shows the resulting time courses, which were fitted best with single exponentials to yield rate constants of 12 ± 1 s^{-1} for PKCα, 48 ± 8 s^{-1} for PKCβ, and 11 ± 2 s^{-1} for PKCγ (Table 2). These rate constants are within 2-fold of those determined for the dissociation of the protein from the ternary complex, implying that Ca^{2+} dissociation occurs on approximately the same time scale as the protein dissociation. Construction of a standard curve by titrating the Quin-2 fluorescence with Ca^{2+} alone allowed determination of the number of Ca^{2+} ions bound in the assembled ternary complex. This experiment revealed that 1.8 ± 0.1 Ca^{2+} ions dissociated from the membrane-bound PKCα ternary complex, 2.8 ± 0.3 Ca^{2+} ions from the PKCβ complex, and 3.2 ± 0.1 Ca^{2+} ions from the PKCγ complex (Figure 9 and Table 1). These stoichiometries are the first measured for the PKCα and

PKCγ ternary complexes, while the stoichiometry measured for the PKCβ ternary complex agrees with the previously published value (4).

DISCUSSION

This side-by-side comparison of the isolated C2 domains from three conventional protein kinase C isoforms, PKCα, PKCβ, and PKCγ, reveals both subtle and significant differences between their Ca^{2+} activation parameters. These domains exhibit similar intrinsic Ca^{2+} affinities, although a greater range of Ca^{2+} affinities is observed in the presence of target membranes, which provide an environment closer to that encountered in cells. The macroscopic rate constants of Ca^{2+} and membrane binding and dissociation also are similar. The most striking difference is in the number of Ca^{2+} ions bound per domain, and in the number and order of the binding events that occur during Ca^{2+}-triggered membrane docking. The latter results provide strong evidence for the specialization of conventional PKC Ca^{2+} activation mechanisms. These differences may have evolved to tune the cooperativity of Ca^{2+} binding in the presence of membranes, which in turn would control the sensitivity of the C2 domain to small changes in the cytoplasmic Ca^{2+} concentration. Moreover, the differences observed between isolated C2 domains may serve to optimize these domains for their different protein contexts, since each C2 domain must act in concert with the specialized C1 and catalytic domains of its PKC isoform (23, 56). In particular, the C1 and C2 domains of conventional PKCs exhibit additive membrane binding (55, 57); thus, the apparent Ca^{2+} and membrane affinities of full-length cPKCs will include additive contributions from both the C1 and C2 domains due to the coupling of Ca^{2+} and membrane binding reactions. Thus, to resolve the regulatory contributions of C1 and C2 domains, a complete, quantitative assessment of the ion and membrane binding characteristics of isolated C2 domains is essential.

Ca^{2+} Activation Affinities, Cooperativities, and Stoichiometries

The isolated C2 domains of PKCα, PKCβ, and PKCγ exhibit similar Ca^{2+} binding affinities in the absence of membranes. Their intrinsic $[Ca^{2+}]_{1/2}$ values, defined as the Ca^{2+} concentration that generates the half-maximal intrinsic tryptophan fluorescence change, range from 18 ± 2 μM for PKCγ, to 35 ± 4 μM for PKCα, to 42 ± 2 μM for PKCβ. The largest differences are in their apparent Hill coefficients for Ca^{2+} binding, which range from 0.9 ± 0.1 for both PKCα and PKCγ to 2.3 ± 0.1 for PKCβ, and in the sign of the Ca^{2+}-triggered fluorescence change, which is negative for PKCα and PKCγ but positive for PKCβ. It follows that the binding of a single Ca^{2+} ion to the PKCα and PKCγ C2 domains generates a different environmental change at the four conserved tryptophan residues than the binding of two or more Ca^{2+} ions to the PKCβ C2 domain.

As expected for a coupled binding equilibrium, the presence of membranes increases the apparent Ca^{2+} affinity of each isolated C2 domain. The degree of affinity enhancement varies among the domains, yielding $[Ca]_{1/2}$ values, defined as the Ca^{2+} concentrations that generate half-maximal protein-to-membrane FRET, ranging from 0.7 ± 0.1 μM for PKCγ, to 1.4 ± 0.1 μM for PKCα, to 5.0 ± 0.2 μM for PKCβ. The effects of membranes on the Ca^{2+} cooperativity also differ significantly for the three C2 domains. The apparent Hill coefficient for Ca^{2+} binding to PKCβ is approximately 2 in the absence and presence of membranes (2.3 ± 0.1 and 1.8 ± 0.1, respectively), suggesting that this domain binds at least two Ca^{2+} ions in both states. In contrast, PKCα and PKCγ exhibit apparent Hill coefficients approaching unity in the absence of membranes (0.9 ± 0.1 for each), suggesting that these isolated domains may only bind a single Ca^{2+} ion. In the presence of membranes, the apparent Hill coefficients of the PKCα and PKCγ domains increase slightly above unity (1.3 ± 0.1 and 1.4 ± 0.1, respectively), suggesting that the number of Ca^{2+} ions bound at micromolar Ca^{2+} concentrations increases from one in solution to greater than one in the

membrane-bound state. For the membrane-bound C2 domain, the phospholipid headgroups could contribute oxygens that directly coordinate Ca^{2+} as seen in the crystal structure of PKCα bound to a short chain PS (17). Such interactions could increase the affinity for Ca^{2+} ions already bound to the isolated C2 domain, or even trigger the binding of additional Ca^{2+} ions to the membrane-bound domain. In turn, the binding of additional Ca^{2+} ions would account for the increased Ca^{2+} cooperativity observed for the PKCα and PKCγ C2 domains in the presence of membranes. Since PKCβ exhibits the highest $[Ca^{2+}]_{1/2}$ values and Hill coefficients in both the absence and presence of membranes, this C2 domain may be designed to be activated at a higher Ca^{2+} concentration but by a smaller fractional change in the Ca^{2+} concentration than the other two isoforms.

The use of Quin-2 and stopped flow kinetics to quantitate Ca^{2+} release enables direct quantitation of the Ca^{2+} stoichiometry of the membrane-bound complex. As published previously and confirmed in the study presented here, PKCβ binds three Ca^{2+} ions in the membrane-docked state (4). Similarly, our study reveals that the PKCγ C2 domain binds three Ca^{2+} ions when docked to membranes. In contrast, only two Ca^{2+} ions are detected for the membrane-bound PKCα C2 domain, indicating that a third Ca^{2+} ion either fails to bind or dissociates too rapidly to detect in the stopped flow analysis. The structural basis for this observed difference in the number of bound Ca^{2+} ions is not yet known, although potential candidate residues are suggested by the primary amino acid sequence as discussed below.

Lipid Stoichiometries

The number of phosphatidylserine lipid molecules interacting with one C2 domain ranges from 3 ± 1 for PKCα, to 4 ± 1 for PKCβ, to 5 ± 1 for PKCγ. Using the crystal structures for PKCα and PKCβ, the area encompassed by the three Ca^{2+} binding loops was determined to range from 130 to 140 $Å^2$ (16, 17). The lipids used here, 1-palmitoyl-2-oleoyl-*sn*-glycero-3-phosphocholine and 1-palmitoyl-2-oleoyl-*sn*-glycero-3-phosphoserine, closely resemble egg yolk phosphatidylcholine (EPC) which is predominantly composed of 16:0 and 18:1 chains. Studies of EPC have provided estimates of the membrane surface area per lipid ranging from 64 to 76 $Å^2$ (as reviewed in ref 58). If an average value of 70 $Å^2$ is assumed, only two lipid headgroups could be sufficient to fill the area encompassed by the Ca^{2+} binding loops. However, three to five lipid headgroups are observed to interact with the C2 domain, suggesting that the interaction surface contains multiple headgroups that are only partially covered by the C2 domain footprint. Interestingly, lipid binding studies have suggested that full-length PKCβII interacts with eight phosphatidylserine molecules and that the C2 domain plays a role in part, but not necessarily all, of this interaction (59).

Kinetics of Ca^{2+} and Membrane Binding

While Ca^{2+} binding and dissociation were too fast to measure for the free C2 domains, the kinetics of membrane docking and dissociation, as well as Ca^{2+} dissociation from the membrane-bound complex, could be measured by stopped flow kinetics. The rate constants for membrane docking are quite similar, ranging from 310 ± 30 s^{-1} for PKCβ, to 420 ± 40 s^{-1} for PKCα, to 440 ± 40 s^{-1} for PKCγ. Thus, at the concentrations used in our study (0.5 μM C2 domain and 250 μM total phospholipid), the Ca^{2+}-activated membrane docking reactions of all three proteins are rate limited by the membrane association event rather than the Ca^{2+} binding event. Additional evidence which shows that membrane association is rate-limiting was provided by the observation that membrane docking kinetics were indistinguishable when Ca^{2+} was placed in either the protein syringe or the membrane syringe prior to stopped flow mixing.

When free Ca^{2+} is removed from the assembled protein–Ca^{2+}–membrane ternary complex by stopped flow mixing with EDTA, an irreversible Ca^{2+} dissociation reaction is triggered

that enables measurement of the kinetics of dissociation of the C2 domain from the membrane. Under these conditions, PKCα remains bound to the membrane more than 3-fold longer than PKCβ, while PKCγ stays docked more than 2-fold longer than PKCβ. If the longer-lived ternary complexes of the PKCα and PKCγ C2 domains yield longer membrane-bound lifetimes for their full-length proteins, these PKC isoforms could have significantly more time for membrane-associated kinase activity. Interestingly, for each ternary complex, the rate constant for Ca^{2+} dissociation was found to be within a factor of 2 of the rate constant for protein dissociation from the membrane, suggesting that Ca^{2+} dissociation occurs simultaneously with or shortly after disruption of the protein–membrane interface.

Models Incorporating Equilibrium and Kinetic Results

To describe the results obtained for the cooperativity, stoichiometry, and kinetics of Ca^{2+}-activated membrane docking, the following general model is proposed: where P represents the C2 domain, L represents the membranes, m represents the number of Ca^{2+} ions that bind prior to membrane docking, and n represents the number of additional Ca^{2+} ions that bind following membrane association.

Our data suggest that PKCβ possesses the highest degree of cooperative Ca^{2+} binding and dissociation. The free PKCβ C2 domain yields an apparent Hill coefficient of 2.3 ± 0.1 for Ca^{2+} binding in the absence of membranes, which is close to the maximum Hill coefficient expected for the binding of two Ca^{2+} ions. This result is consistent with the model previously proposed by Nalefski and Newton (57) in which two Ca^{2+} ions are proposed to rapidly bind to the isolated domain, followed by slow membrane docking and the binding of the third Ca^{2+} ion such that $m = 2$ and $n = 1$ in Scheme 1. The ability of this domain to bind up to three Ca^{2+} ions is supported by crystallographic and modeling studies revealing that three Ca^{2+} ions bind to the free domain at millimolar Ca^{2+} concentrations; such high Ca^{2+} levels are able to drive the binding of the third Ca^{2+} ion even in the absence of membranes (16, 69). For this C2 domain, the kinetics of membrane docking upon Ca^{2+} addition and of membrane dissociation upon Ca^{2+} removal are both monoexponential, suggesting a single rate-limiting step in both directions (present results and refs 4 and 57). The dissociation of Ca^{2+} from the membrane-bound complex is also monoexponential and exhibits a time constant indistinguishable from that of membrane dissociation (present results and ref 4). Thus, the available evidence for the forward reaction indicates that the slow membrane association (k_2 in step 2) is rate-limiting relative to the prior and subsequent Ca^{2+} binding steps (k_1 and k_3 in steps 1 and 3, respectively). In contrast, the available evidence for the reverse reaction suggests that the dissociation of the Ca^{2+} ion that was last to bind (k_{-3} in step 3) is rate-limiting such that the subsequent dissociation of the protein from the membrane and the release of the final two Ca^{2+} ions are relatively fast.

The Hill coefficients observed for Ca^{2+} binding to the free PKCα and PKCγ C2 domains (both 0.9 ± 0.1) suggest that only one Ca^{2+} ion binds prior to membrane docking such that $m = 1$ in step 1 of Scheme 1. After membrane docking, at least one additional Ca^{2+} ion binds to the membrane-bound PKCα C2 domain ($n = 1$), while two additional Ca^{2+} ions bind to the membrane-docked PKCγ C2 domain ($n = 2$), as indicated in step 3 of Scheme 1. Again, monoexponential kinetics are observed for both the membrane docking and membrane dissociation reactions of these C2 domains. These monoexponential kinetics are consistent with the same rate-limiting steps proposed for the PKCβ C2 domain: membrane association (k_2 in step 2) in the forward reaction and dissociation of the last-to-bind Ca^{2+} ion or ions in the reverse direction (k_{-3} in step 3).

Interestingly, the measured Ca^{2+} stoichiometries observed in crystal structures of the isolated PKCα and PKCβ C2 domains range from two to three Ca^{2+} ions per domain (16,

17, 41). These stoichiometries are higher than those proposed to occur prior the docking of cPKC C2 domains to membranes in the above model. This apparent contradiction is explained by the high Ca^{2+} concentrations used during crystallization (from 2 to 12 mM). In the simplest picture, the physiologically relevant micromolar Ca^{2+} concentrations fail to load at least one Ca^{2+} site prior to membrane docking, while millimolar Ca^{2+} concentrations can load additional Ca^{2+} sites in the absence of membranes. For the PKCβ C2 domain, the three Ca^{2+} ions observed in the crystal structure likely correspond to the same three Ca^{2+} ions detected in the membrane-bound ternary complex (ref 4 and present results). For the PKCα C2 domain, the two Ca^{2+} ions detected in the membrane-bound ternary complex appear to match the two Ca^{2+} ions observed in an earlier crystal structure of a ternary complex between the C2 domain, Ca^{2+} ions, and a short chain PS analogue (17). However, a more recent crystal structure of a ternary complex containing the PKCα C2 domain and a different short chain PS analogue reveals three bound Ca^{2+} ions (41). The fact that the latter structure contains a third Ca^{2+} ion not detected in the membrane-bound ternary complex could arise from artificial loading of a physiologically irrelevant site by the high Ca^{2+} concentration during crystallization (12 mM). Alternatively, the weakly bound third ion may dissociate too rapidly to detect in the present quantitation of Ca^{2+} ions in the membrane-bound complex, since only those ions that dissociate more slowly than the dead time of the stopped flow instrument (0.9 ms) will be observed. In either case, the affinity of the PKCα C2 domain for a third Ca^{2+} ion is significantly lower than that of the PKCβ and PKCγ C2 domains, which both stably bind a third Ca^{2+} ion in the membrane-bound complex.

Analysis of the Primary Amino Acid Sequence

An analysis of the primary amino acid sequence between the PKCα, PKCβ, and PKCγ C2 domains reveals that 62% of their residues are identical (see Figure 1), indicating considerable homology. To identify the primary structure differences underlying the different affinities of these C2 domains for a third Ca^{2+} ion, it is useful to focus on the three interstrand loops, termed Ca^{2+} binding loops 1–3 (CBL 1–3), which have been previously implicated in both Ca^{2+} coordination and direct contacts with the membrane surface for these and other C2 domains (8–17, 60–64). CBL 1 is identical in the PKCα, PKCβ, and PKCγ C2 domains except for a single change which is not correlated with the observed Ca^{2+} stoichiometries. Although in other C2 domains CBL 2 provides direct Ca^{2+} coordination (8–10, 14, 15), the crystal structures of PKCα and PKCβ reveal no direct Ca^{2+} coordination by this loop which exhibits four substitutions, including two nonconservative substitutions (16, 17). In other C2 domains, CBL 2 also plays the least important role in membrane docking (64, 65). However, the Arg at CBL 2 position 216 in PKCα is replaced with Lys in PKCβ and PKCγ; thus, the Arg may be responsible for repulsive interactions with the third Ca^{2+} ion that are reduced by the lower pK_a of Lys. Finally, CBL 3 exhibits two substitutions, only one of which is correlated with the observed Ca^{2+} stoichiometries. At position 251 of CBL 3, a Thr in PKCα is conservatively changed to a Ser in PKCβ and -γ. This residue is critical for the Ca^{2+}-triggered membrane docking and enzymatic activation of full-length PKCα, and directly coordinates the third Ca^{2+} ion when it is present in crystal structures of PKC C2 domains (16, 41, 63). While the differences between the Thr and Ser side chains are subtle, the extra methyl group may significantly lower the affinity of PKCα for the third Ca^{2+} ion in the membrane-bound state. In short, although positions 216 and 251 are the most likely candidates, further studies are required to identify the structural features of PKCα that underlie its lower or negligible affinity for a third Ca^{2+} ion in the membrane-docked state.

Implications for PKC Signaling in vivo

Overall, the equilibrium and kinetic data presented herein suggest that conventional PKC isoforms may respond to different levels of Ca^{2+} transients in the cellular environment.

Although previous studies have measured the $[Ca^{2+}]_{1/2}$ values for activation of kinase activity in the full-length PKCα and PKCβ enzymes, the use of significantly different membrane and diacylglycerol concentrations in different laboratories prevents direct comparisons of these parameters (66, 67). Thus, quantitative, side-by-side studies of the full-length enzymes must be undertaken to ascertain whether differences between their C2 domains dominate the membrane docking reaction. If it is assumed that the C1 domains of conventional PKCs exhibit equivalent interactions with the membrane, the relative Ca^{2+} activation parameters measured in our study for isolated C2 domains predict that a large Ca^{2+} transient would induce docking of all three C2 domains at a similar rate. During a small Ca^{2+} transient, PKCγ would dock more efficiently than PKCα, which in turn would dock more efficiently than PKCβ. Once docked to the membrane, PKCα would remain longer than PKCγ, which in turn would remain longer than PKCβ. These contrasting activation and inactivation parameters are proposed to be required for the specialized functions of conventional PKC isoforms in different PKC signaling pathways.

Even more dramatic differences are observed between C2 domains from different functional classes. The isolated C2 domains from conventional PKCs, synaptotagmin I and cytosolic phospholipase A2, exhibit widely varying $[Ca^{2+}]_{1/2}$ values, membrane binding and dissociation kinetics, and mechanisms of membrane association (4). Of these C2 domains, the PKCα, -β, and -γ isoforms exhibit properties most similar to those of the C2A domain of synaptotagmin I, which also exhibits an ionic mechanism of membrane docking and prefers anionic phospholipids but is activated at significantly higher Ca^{2+} concentrations and possesses significantly faster membrane binding and dissociation kinetics than the PKC C2 domains. In contrast, the C2 domain of cytosolic phospholipase A2 exhibits a hydrophobic docking mechanism and prefers neutral phospholipids, and this C2 domain also exhibits much slower membrane binding and dissociation kinetics than the synaptotagmin I C2A and PKCα, -β, and -γ C2 domains. In some cases, the physiological role of a C2 domain provides a simple explanation for its specialized activation parameters; for example, the high Ca^{2+} concentration needed to activate the synaptotagmin I C2A domain is consistent with the high Ca^{2+} fluxes achieved at the synapse, and the rapid activation kinetics of this domain are consistent with its proposed role as the trigger for neurotransmitter release (68). In other cases, further study is needed to elucidate the physiological driving forces that underlie the evolution of dramatic C2 domain specializations.

Acknowledgments

We thank the following for their kind gifts of cDNA: Professors Ohno and Nishizuka (PKCα, Kobe, Japan) and Professor Tobias Meyer (PKCγ, Stanford University, Stanford, CA).

REFERENCES

1. Berridge MJ, Bootman MD, Lipp P. Nature. 1998; 395:645–648. [PubMed: 9790183]
2. Spitzer NC, Lautermilch NJ, Smith RD, Gomez TM. BioEssays. 2000; 22:811–817. [PubMed: 10944583]
3. Falke JJ, Drake SK, Hazard AL, Peersen OB. Q. Rev. Biophys. 1994; 27:219–290. [PubMed: 7899550]
4. Nalefski EA, Wisner MA, Chen JZ, Sprang SR, Fukuda M, Mikoshiba K, Falke JJ. Biochemistry. 2001; 40:3089–3100. [PubMed: 11258923]
5. Nalefski EA, Falke JJ. Protein Sci. 1996; 5:2375–2390. [PubMed: 8976547]
6. Rizo J, Sudhof TC. J. Biol. Chem. 1998; 273:15879–15882. [PubMed: 9632630]
7. Hurley JH, Misra S. Annu. Rev. Biophys. Biomol. Struct. 2000; 29:49–79. [PubMed: 10940243]
8. Perisic O, Fong S, Lynch DE, Bycroft M, Williams RL. J. Biol. Chem. 1998; 273:1596–1604. [PubMed: 9430701]

9. Xu GY, McDonagh T, Yu HA, Nalefski EA, Clark JD, Cumming DA. J. Mol. Biol. 1998; 280:485–500. [PubMed: 9665851]
10. Dessen A, Tang J, Schmidt H, Stahl M, Clark JD, Seehra J, Somers WS. Cell. 1999; 97:349–360. [PubMed: 10319815]
11. Sutton RB, Davletov BA, Berghuis AM, Sudhof TC, Sprang SR. Cell. 1995; 80:929–938. [PubMed: 7697723]
12. Shao X, Fernandez I, Sudhof TC, Rizo J. Biochemistry. 1998; 37:16106–16115. [PubMed: 9819203]
13. Sutton RB, Ernst JA, Brunger AT. J. Cell Biol. 1999; 147:589–598. [PubMed: 10545502]
14. Essen LO, Perisic O, Cheung R, Katan M, Williams RL. Nature. 1996; 380:595–602. [PubMed: 8602259]
15. Grobler JA, Essen LO, Williams RL, Hurley JH. Nat. Struct. Biol. 1996; 3:788–795. [PubMed: 8784353]
16. Sutton RB, Sprang SR. Structure. 1998; 6:1395–1405. [PubMed: 9817842]
17. Verdaguer N, Corbalan-Garcia S, Ochoa WF, Fita I, Gomez-Fernandez JC. EMBO J. 1999; 18:6329–6338. [PubMed: 10562545]
18. Pappa H, Murray-Rust J, Dekker LV, Parker PJ, McDonald NQ. Structure. 1998; 6:885–894. [PubMed: 9687370]
19. Ochoa WF, Garcia-Garcia J, Fita I, Corbalan-Garcia S, Verdaguer N, Gomez-Fernandez JC. J. Mol. Biol. 2001; 311:837–849. [PubMed: 11518534]
20. Lee JO, Yang H, Georgescu MM, Di Cristofano A, Maehama T, Shi Y, Dixon JE, Pandolfi P, Pavletich NP. Cell. 1999; 99:323–334. [PubMed: 10555148]
21. Walker EH, Perisic O, Ried C, Stephens L, Williams RL. Nature. 1999; 402:313–320. [PubMed: 10580505]
22. Hofmann J. FASEB J. 1997; 11:649–669. [PubMed: 9240967]
23. Newton AC. Chem. Rev. 2001; 101:2353–2364. [PubMed: 11749377]
24. Nishizuka Y. FASEB J. 1995; 9:484–496. [PubMed: 7737456]
25. Cornford P, Evans J, Dodson A, Parsons K, Woolfenden A, Neoptolemos J, Foster CS. Am. J. Pathol. 1999; 154:137–144. [PubMed: 9916928]
26. Dean N, McKay R, Miraglia L, Howard R, Cooper S, Giddings J, Nicklin P, Meister L, Ziel R, Geiger T, Muller M, Fabbro D. Cancer Res. 1996; 56:3499–3507. [PubMed: 8758918]
27. Bowling N, Walsh RA, Song G, Estridge T, Sandusky GE, Fouts RL, Mintze K, Pickard T, Roden R, Bristow MR, Sabbah HN, Mizrahi JL, Gromo G, King GL, Vlahos CJ. Circulation. 1999; 99:384–391. [PubMed: 9918525]
28. Wakasaki H, Koya D, Schoen FJ, Jirousek MR, Ways DK, Hoit BD, Walsh RA, King GL. Proc. Natl. Acad. Sci. U.S.A. 1997; 94:9320–9325. [PubMed: 9256480]
29. Basbaum AI. Proc. Natl. Acad. Sci. U.S.A. 1999; 96:7739–7743. [PubMed: 10393891]
30. Martin WJ, Malmberg AB, Basbaum AI. J. Neurosci. 2001; 21:5321–5327. [PubMed: 11438608]
31. Hofmann J. Rev. Physiol. Biochem. Pharmacol. 2001; 142:1–96. [PubMed: 11190577]
32. Boesch DM, Garvin JL. Am. J. Physiol. 2001; 281:R861–R867.
33. Csukai M, Mochly-Rosen D. Pharmacol. Res. 1999; 39:253–259. [PubMed: 10208754]
34. Ron D, Chen CH, Caldwell J, Jamieson L, Orr E, Mochly-Rosen D. Proc. Natl. Acad. Sci. U.S.A. 1994; 91:839–843. [PubMed: 8302854]
35. Csukai M, Chen CH, De Matteis MA, Mochly-Rosen D. J. Biol. Chem. 1997; 272:29200–29206. [PubMed: 9360998]
36. Ron D, Luo J, Mochly-Rosen D. J. Biol. Chem. 1995; 270:24180–24187. [PubMed: 7592622]
37. Stebbins EG, Mochly-Rosen D. J. Biol. Chem. 2001; 276:29644–29650. [PubMed: 11387319]
38. Knopf JL, Lee MH, Sultzman LA, Kriz RW, Loomis CR, Hewick RM, Bell RM. Cell. 1986; 46:491–502. [PubMed: 3755379]
39. Ono Y, Fujii T, Igarashi K, Kikkawa U, Ogita K, Nishizuka Y. Nucleic Acids Res. 1988; 16:5199–5200. [PubMed: 3387228]

40. Housey GM, Johnson MD, Hsiao WL, O'Brian CA, Murphy JP, Kirschmeier P, Weinstein IB. Cell. 1988; 52:343–354. [PubMed: 3345563]
41. Ochoa WF, Corbalan-Garcia S, Eritja R, Rodriguez-Alfaro JA, Gomez-Fernandez JC, Fita I, Verdaguer N. J. Mol. Biol. 2002; 320:277–291. [PubMed: 12079385]
42. Murray D, Honig B. Mol. Cell. 2002; 9:145–154. [PubMed: 11804593]
43. Needham JV, Chen TY, Falke JJ. Biochemistry. 1993; 32:3363–3367. [PubMed: 8461299]
44. Gill SC, von Hippel PH. Anal. Biochem. 1989; 182:319–326. [PubMed: 2610349]
45. Smith PK, Krohn RI, Hermanson GT, Mallia AK, Gartner FH, Provenzano MD, Fujimoto EK, Goeke NM, Olson BJ, Klenk DC. Anal. Biochem. 1985; 150:76–85. [PubMed: 3843705]
46. Laemmli UK. Nature. 1970; 227:680–685. [PubMed: 5432063]
47. Careaga CL, Falke JJ. J. Mol. Biol. 1992; 226:1219–1235. [PubMed: 1518053]
48. Bryant DT. Biochem. J. 1985; 226:613–616. [PubMed: 3994676]
49. Linse S, Helmersson A, Forsen S. J. Biol. Chem. 1991; 266:8050–8054. [PubMed: 1902469]
50. Hazard AL, Kohout SC, Stricker NL, Putkey JA, Falke JJ. Protein Sci. 1998; 7:2451–2459. [PubMed: 9828012]
51. Nalefski EA, McDonagh T, Somers W, Seehra J, Falke JJ, Clark JD. J. Biol. Chem. 1998; 273:1365–1372. [PubMed: 9430670]
52. Creighton, TE. Proteins: structures and molecular properties. 2nd ed.. New York: W. H. Freeman; 1993.
53. Peersen OB, Madsen TS, Falke JJ. Protein Sci. 1997; 6:794–807. [PubMed: 9098889]
54. Nalefski EA, Slazas MM, Falke JJ. Biochemistry. 1997; 36:12011–12018. [PubMed: 9340010]
55. Johnson JE, Giorgione J, Newton AC. Biochemistry. 2000; 39:11360–11369. [PubMed: 10985781]
56. Hurley JH, Meyer T. Curr. Opin. Cell Biol. 2001; 13:146–152. [PubMed: 11248547]
57. Nalefski EA, Newton AC. Biochemistry. 2001; 40:13216–13229. [PubMed: 11683630]
58. Nagle JF, Tristram-Nagle S. Biochim. Biophys. Acta. 2000; 1469:159–195. [PubMed: 11063882]
59. Mosior M, Newton AC. Biochemistry. 1998; 37:17271–17279. [PubMed: 9860841]
60. Chae YK, Abildgaard F, Chapman ER, Markley JL. J. Biol. Chem. 1998; 273:25659–25663. [PubMed: 9748232]
61. Nalefski EA, Falke JJ. Biochemistry. 1998; 37:17642–17650. [PubMed: 9922129]
62. Medkova M, Cho W. J. Biol. Chem. 1998; 273:17544–17552. [PubMed: 9651347]
63. Conesa-Zamora P, Lopez-Andreo MJ, Gomez-Fernandez JC, Corbalan-Garcia S. Biochemistry. 2001; 40:13898–13905. [PubMed: 11705379]
64. Frazier AA, Wisner MA, Malmberg NJ, Victor KG, Fanucci GE, Nalefski EA, Falke JJ, Cafiso DS. Biochemistry. 2002; 41:6282–6292. [PubMed: 12009889]
65. Ball A, Nielsen R, Gelb MH, Robinson BH. Proc. Natl. Acad. Sci. U.S.A. 1999; 96:6637–6642. [PubMed: 10359764]
66. Bittova L, Stahelin RV, Cho W. J. Biol. Chem. 2001; 276:4218–4226. [PubMed: 11029472]
67. Edwards AS, Newton AC. Biochemistry. 1997; 36:15615–15623. [PubMed: 9398289]
68. Brose N, Petrenko AG, Sudhof TC, Jahn R. Science. 1992; 256:1021–1025. [PubMed: 1589771]
69. Banci L, Cavallaro G, Kheifets V, Mochly-Rosen D. J. Biol. Chem. 2002; 277:12988–12997. [PubMed: 11782454]

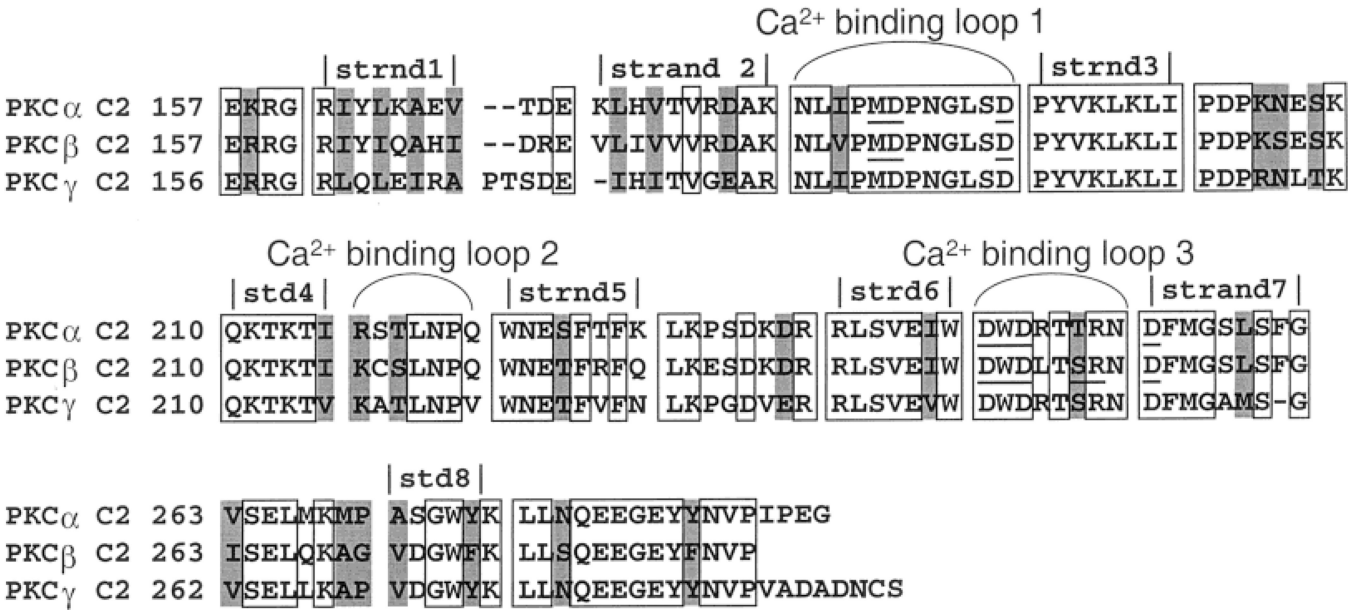

Figure 1.

Primary amino acid sequence alignment for the isolated C2 domains of PKCα, PKCβ, and PKCγ. Loops and β sheets are assigned according to the designations of the PKCα and PKCβ crystal structures (16, 17). Light gray boxes indicate homologous residues; open boxes denote identical residues, and the coordinating residues of the PKCα and PKCβ crystal structures are underlined.

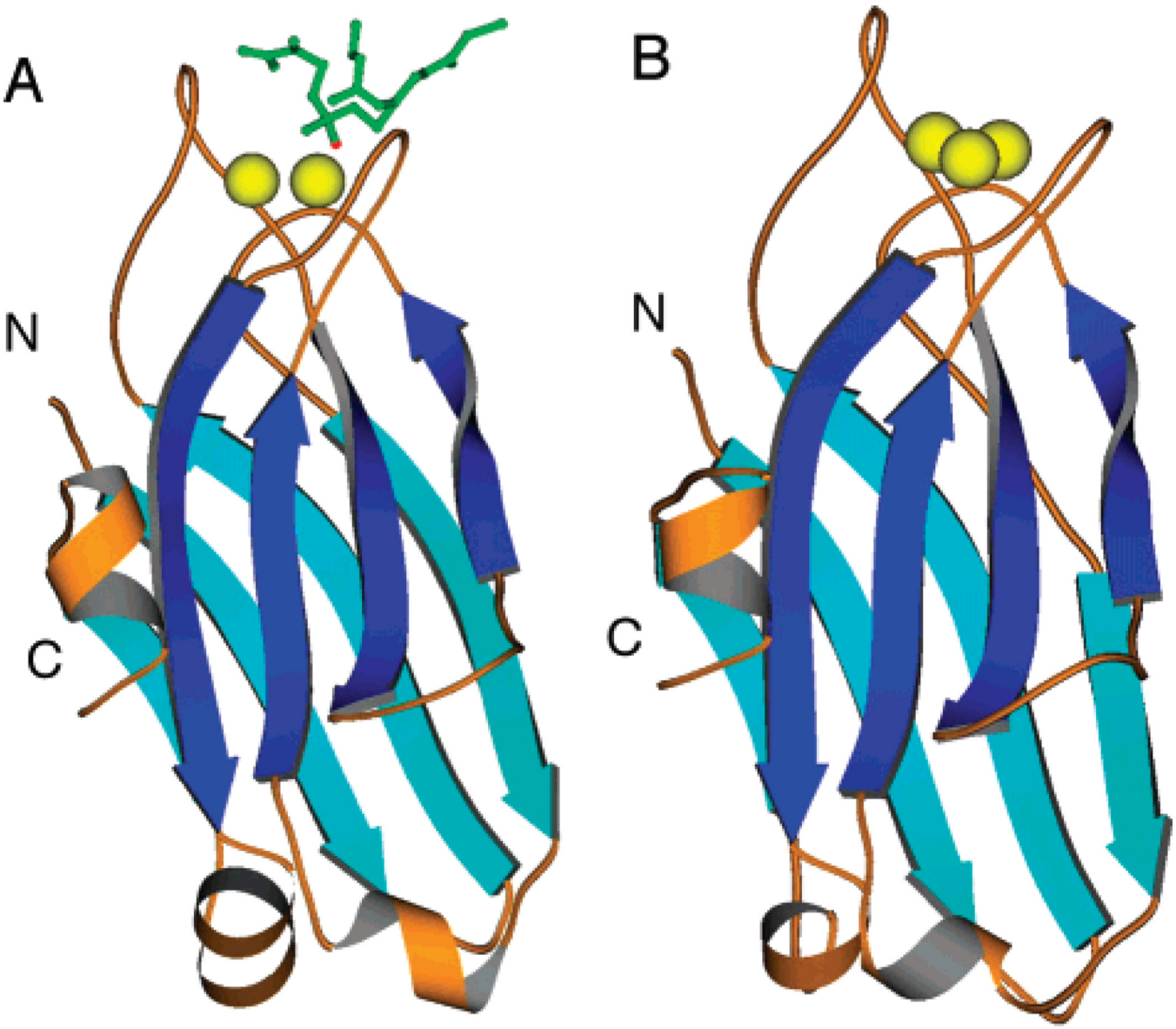

Figure 2.
Available X-ray crystal structures. (A) PKCα (17) and (B) PKCβ (16) isolated C2 domains. The PKCα structure was cocrystallized in the presence of the short chain lipid 1,2-dicaproyl-*sn*-phosphatidyl-L-serine (DCPS) shown in green. A coordinating phosphate oxygen from the DCPS is shown in red. Ca^{2+} ions are shown in yellow.

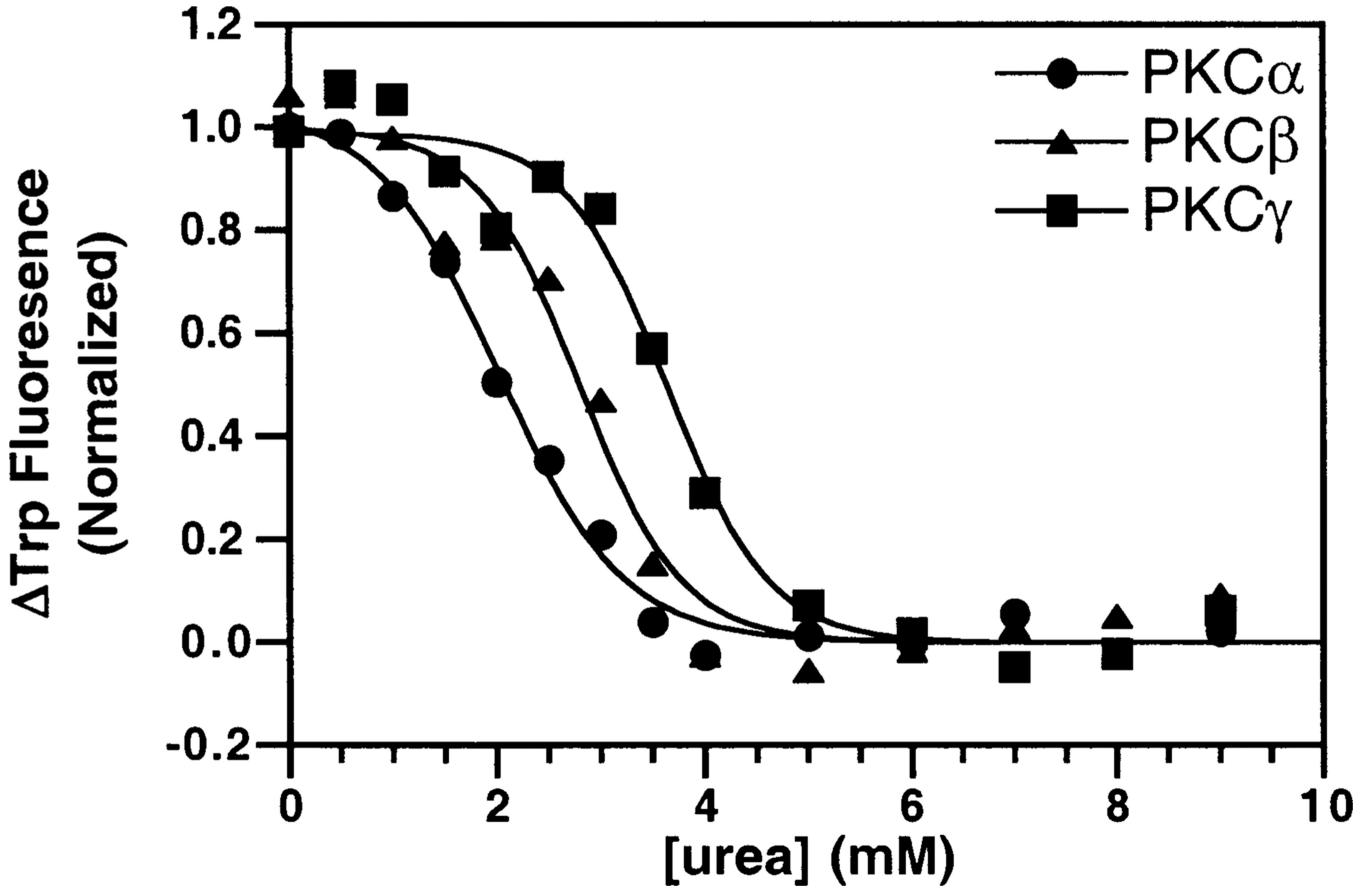

Figure 3.

Urea denaturation of the isolated, Ca^{2+}-free C2 domains. Urea was titrated into a solution with 0.5 μM PKCα (●), PKCβ (▲), or PKCγ (■) and 1 mM EDTA. The resulting change in the intrinsic tryptophan fluorescence was monitored. Data were fit by eq 1. Experimental conditions: 25 °C, 20 mM HEPES (pH 7.4), 100 mM KCl, and 5 mM DTT.

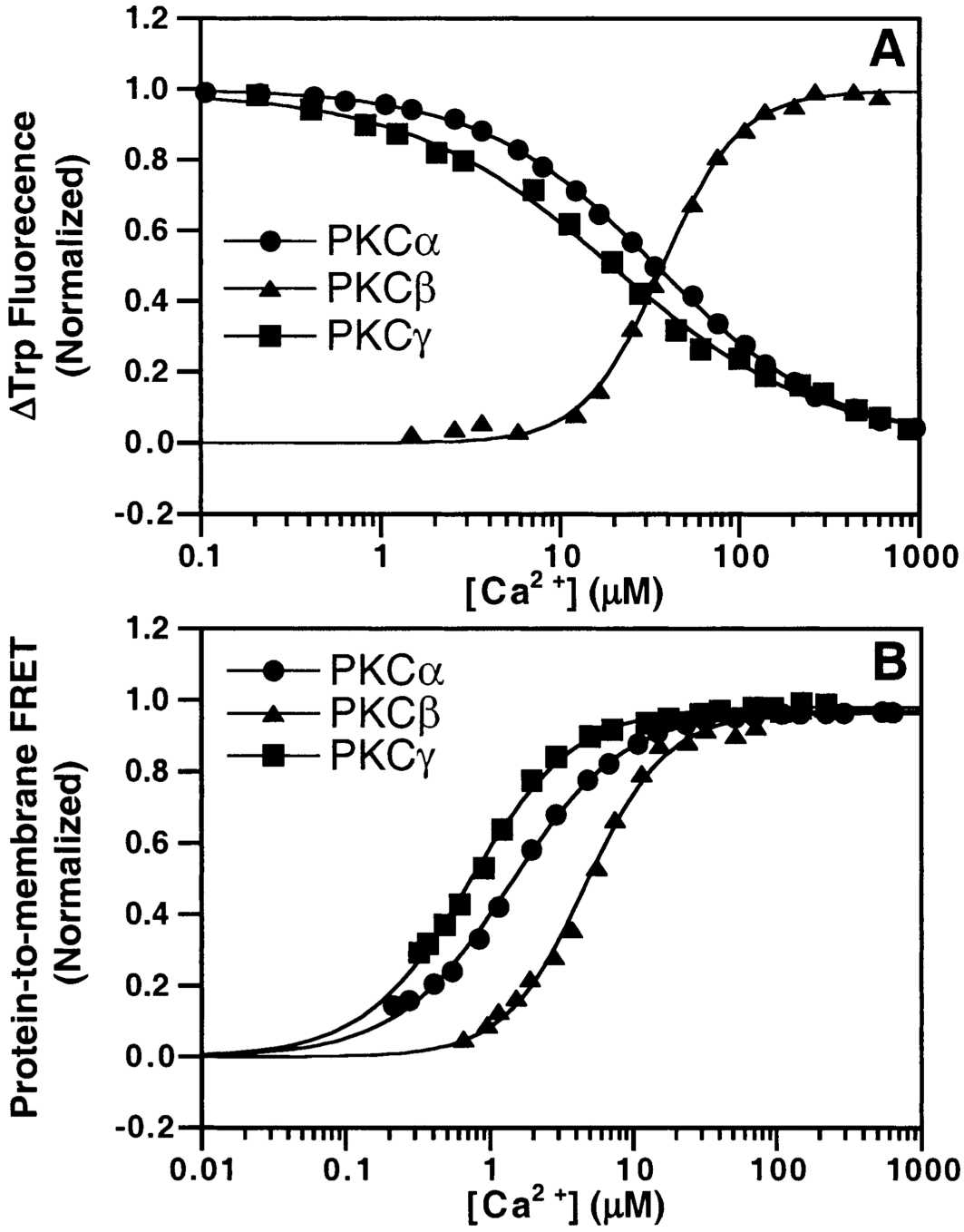

Figure 4.

Ca^{2+} affinities of PKC C2 domains. Ca^{2+} was titrated into solutions containing 0.5 μM PKCα (●), PKCβ (▲), or PKCγ (■) C2 domains in the absence (A) or presence (B) of PC/PS/dPE (47.5%:47.5%:5% mole percent) vesicles. Ca^{2+} binding to isolated C2 domain was monitored by the intrinsic Trp fluorescence. Membrane docking was assessed by monitoring the intrinsic Trp quenching due to protein-to-membrane FRET. The free Ca^{2+} concentration in the presence of membranes was monitored with magnesium green (eq 2), a fluorescent chelator. Solid lines indicate the best fit of the resulting normalized FRET signals to the Hill equation (eq 4). Experimental conditions: 25 °C, 20 mM HEPES (pH 7.4), 100 mM KCl, 5 mM DTT, and 250 μM phospholipid.

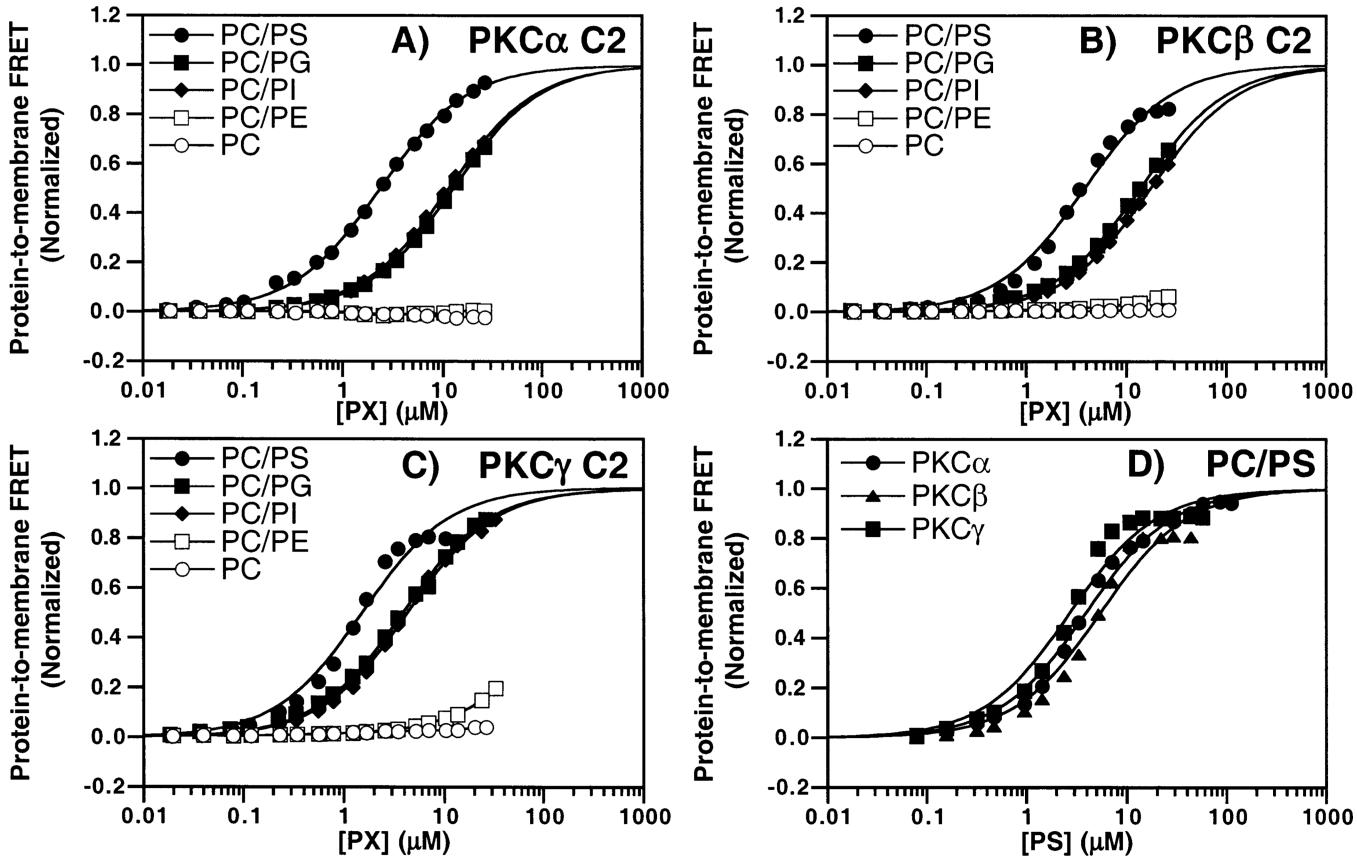

Figure 5.

Phospholipid headgroup specificity of C2 domains. Phospholipid was titrated into solutions containing 0.5 μM PKCα (A), PKCβ (B), or PKCγ (C) C2 domains. Vesicles were composed of a 3:1 PC/PX/dPE mixture (72.5%:22.5%:5% mole percent) where PX is PS (●), PG (■), PI (◆), PE (□), or PC alone (○). Best-fit apparent K_D values were determined for binding to membranes containing PS, PG, and PI (but not PE or PC due to insufficient affinity). These apparent K_D values were 3 ± 1, 13 ± 2, and 11 ± 3 for the PKCα C2 domain, 4 ± 1, 14 ± 2, and 17 ± 3 for the PKCβ C2 domain, and 2 ± 1, 5 ± 1, and 4 ± 1 for the PKCγ C2 domain binding to PS, PG, and PI membranes, respectively. (D) Comparison of PKCα, PKCβ, and PKCγ C2 domain docking to PC/PS/dPE membranes (47.5%: 47.5%: 5% mole percent). Protein docking was assessed by protein-to-membrane FRET, using acceptor fluorescence to quantitate the FRET. Solid lines represent the best fit of the resulting normalized FRET signal to the independent single-site fit (eq 3). In all experiments, the indicated lipid concentrations were obtained by dividing the total lipid concentration by a factor of 2, thereby yielding the lipid concentration arising from the accessible outer leaflets of the vesicles. Experimental conditions: 25 °C, 1 mM free Ca^{2+}, 100 mM KCl, 20 mM HEPES (pH 7.4), and 5 mM DTT.

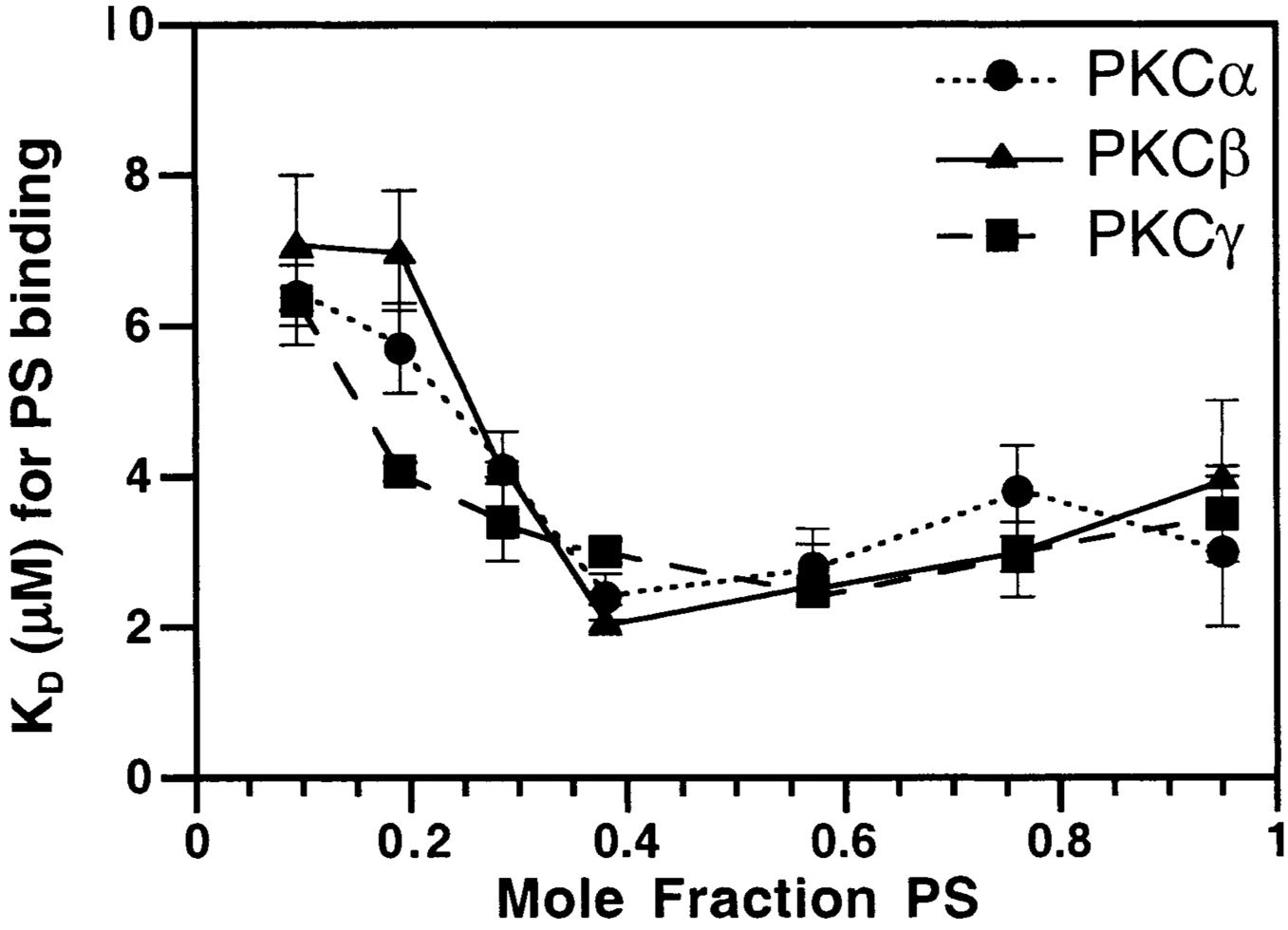

Figure 6.

Phosphatidylserine dependence of C2 domain docking. Increasing percentages of PS in PC/PS/dPE mixtures were titrated into solutions containing C2 domains. The change in the protein-to-membrane FRET as the concentration of PS varied was fit with the independent site model (eq 3). The resulting dissociation constants were plotted vs the increasing percentages of PS for PKCα (●), PKCβ (▲), and PKCγ (■) C2 domains. Protein docking was assessed by protein-to-membrane FRET, using acceptor fluorescence to quantitate the FRET. The dissociation constant calculations used the total PS concentration divided by 2, to focus on lipids in the accessible outer leaflets of vesicles. Experimental conditions: 25 °C, 1 mM free Ca^{2+}, 100 mM KCl, 20 mM HEPES (pH 7.4), and 5 mM DTT.

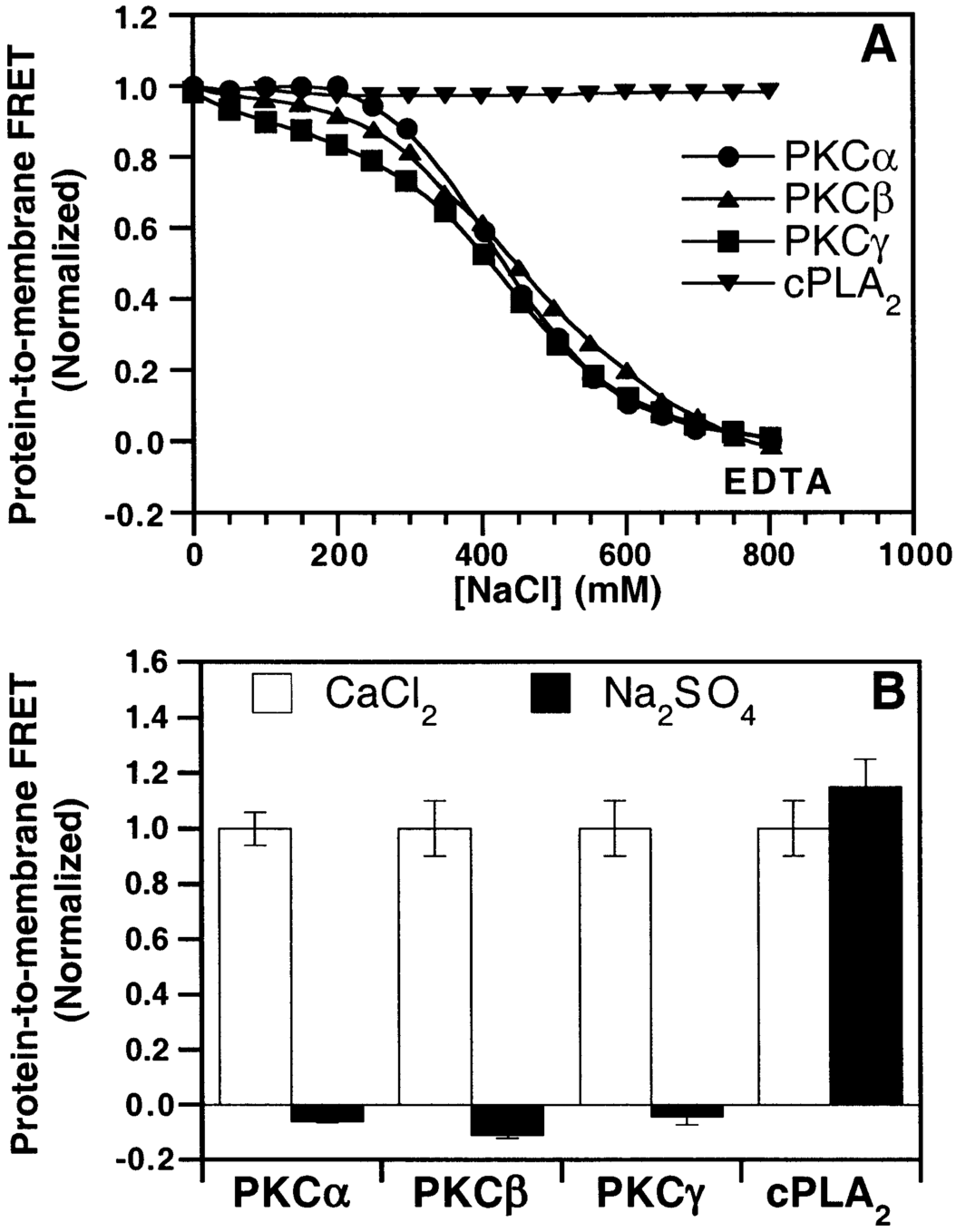

Figure 7.

Ionic strength dependence of membrane docking. (A) NaCl was titrated into a solution of PKCα (●), PKCβ (▲), PKCγ (■), or cytosolic phospholipase A2 (▼), also containing 1 mM free Ca^{2+} and PC/PS/dPE (47.5%:47.5%:5% mole percent) vesicles. Protein docking was assessed by protein-to-membrane FRET, using acceptor fluorescence to quantitate the FRET. The FRET signal was normalized to the initial FRET signal in the absence of added NaCl. EDTA was added to demonstrate that any remaining protein–membrane interaction had been completely disrupted. (B) The indicated C2 domain and PC/PS/dPE (47.5%: 47.5%:5% mole percent) vesicles were incubated with 1.9 M Na_2SO_4 and 5 mM EDTA (black bars) or 2 mM $CaCl_2$ and 1 mM EDTA (white bars). The resulting FRET signals

were normalized to the Ca^{2+}-triggered FRET signals. Cytosolic phospholipase A2 data were taken from Nalefski et al. (4). Experimental conditions: 25 °C, 250 μM lipid, 100 mM KCl, 20 mM HEPES (pH 7.4), and 5 mM DTT.

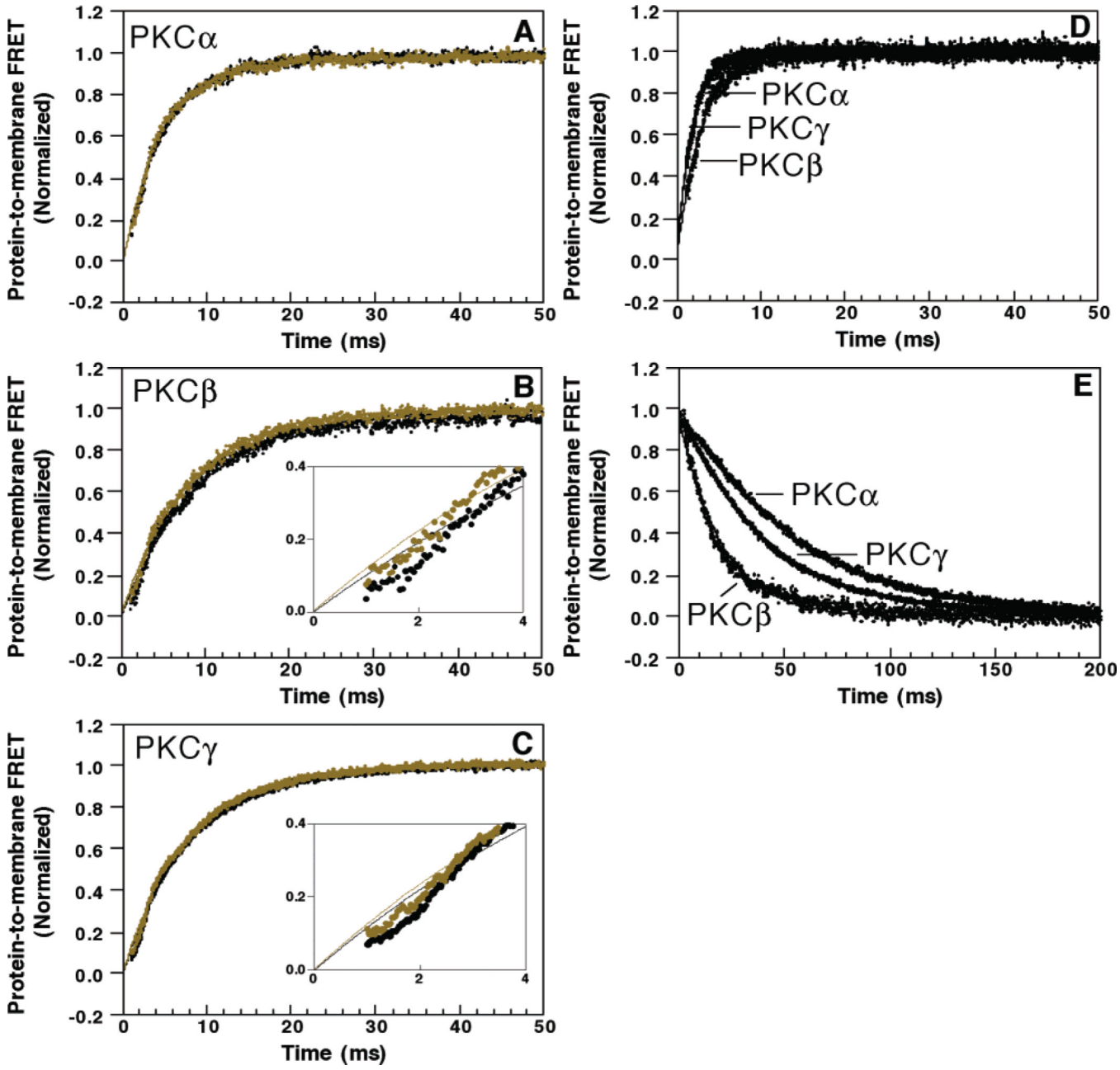

Figure 8.

Kinetics of C2 domain activation and dissociation. (A–C) Ca^{2+}-triggered docking of the C2 domain to membranes was initiated by stopped flow mixing the indicated C2 domain, either premixed with Ca^{2+} (green) or not (black), with an equal volume of PC/PS/dPE (47.5%:47.5%:5% mole percent, 250 μM) vesicles and 1 mM free Ca^{2+}. Insets for panels B and C show the first 4 ms of the traces. (D) The above experiment was repeated in a side-by-side comparison of the three domains by mixing a solution containing the indicated C2 domain and 1 mM free Ca^{2+} with an equal volume of PC/PS/dPE (47.5%:47.5%:5% mole percent, 500 μM) vesicles. (E) C2 domain dissociation from PC/PS/dPE membranes (47.5%:47.5%:5% mole percent) was initiated by mixing with an equal volume of EDTA (10 mM), which chelates the free Ca^{2+}, thereby making the membrane dissociation irreversible. Protein

docking and dissociation were assessed using the acceptor fluorescence to quantitate protein-to-membrane FRET. Solid lines, which in some cases are hidden under the data, indicate the best fit to a single-exponential equation. Experimental conditions: 25 °C, 100 mM KCl, 20 mM HEPES (pH 7.4), and 5 mM DTT.

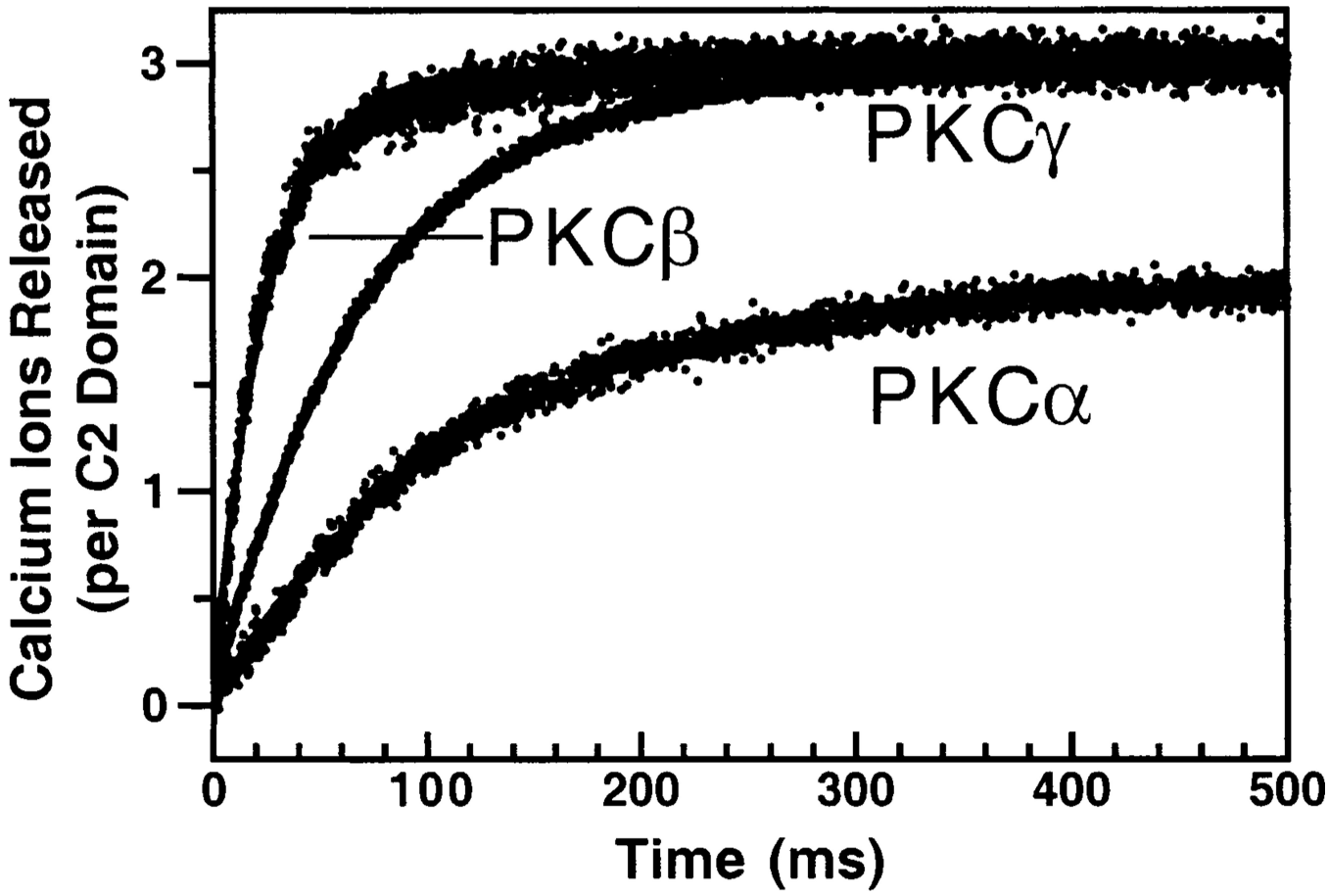

Figure 9.

Determination of the Ca^{2+} stoichiometry for the membrane-bound complex. Ca^{2+} release from the C2 domain complexed with membrane was initiated by stopped flow mixing a solution containing the preformed complex of the C2 domain, Ca^{2+} (100 μM), and PC/PS (50%:50% mole percent, 500 μM phospholipid) vesicles with an equal volume of the fluorescent Ca^{2+} chelator Quin-2 (200 μM). The slow release of Ca^{2+} ions from the complex was quantitated from the increase in the Quin-2 emission. Solid lines represent the best fit of the resulting normalized Quin-2 signals to a single-exponential equation. For each experiment, a Quin-2 standard curve was used to calibrate the number of Ca^{2+} ions that were released. Experimental conditions: 25 °C, 100 mM KCl, 20 mM HEPES (pH 7.4), and 5 mM DTT.

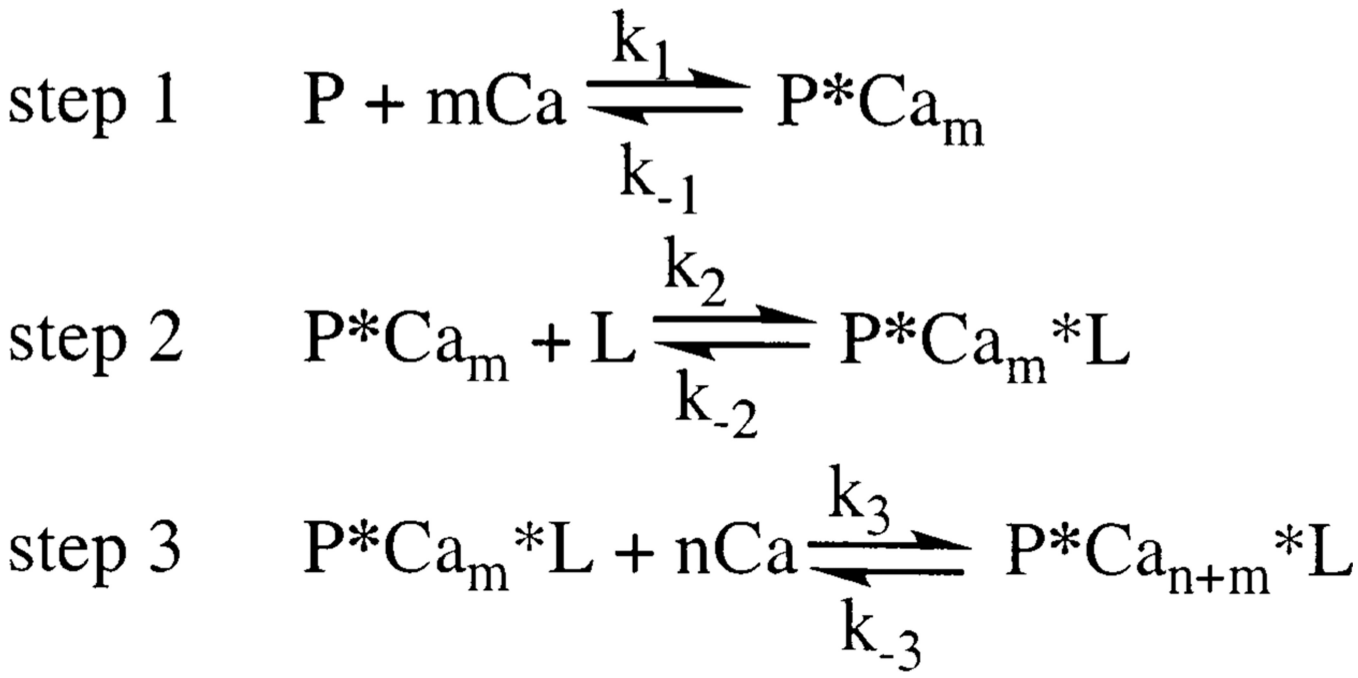

Scheme 1.

Table 1

Comparison of Equilibrium, Stability, and Ligand Binding Parameters

	stability	intrinsic Ca^{2+} binding		Ca^{2+} dependence of membrane binding		phospholipid affinity	phospholipid stoichiometry	Ca^{2+} stoichiometry
C2 domain	$\Delta G_{unfolding}$ (kJ/mol)	$[Ca^{2+}]_{1/2}$ (μM)	Hill coefficient	$[Ca^{2+}]_{1/2}$ (μM)	Hill coefficient	K_D (μM)	no. of phospholipids per C2 domain	no. of Ca^{2+} ions per C2 domain
PKCα	8	35 ± 4	0.9 ± 0.1	1.4 ± 0.1	1.3 ± 0.1	3.0 ± 0.2	3 ± 1	1.8 ± 0.1
PKCβ	14	42 ± 2	2.3 ± 0.1	5.0 ± 0.2	1.8 ± 0.1	4.4 ± 0.4	4 ± 1	2.8 ± 0.3
PKCγ	18	18 ± 2	0.9 ± 0.1	0.7 ± 0.1	1.4 ± 0.1	3.1 ± 0.5	5 ± 1	3.2 ± 0.1

Table 2

Comparison of Kinetic Parameters

	membrane association	membrane dissociation	Ca^{2+} dissociation
C2 domain	**k_1(app) (s^{-1})**	**k_{-1} (s^{-1})**	**k_{off} (s^{-1})**
PKCα	420 ± 40	17.3 ± 0.7	12 ± 1
PKCβ	310 ± 30	57 ± 7	48 ± 8
PKCγ	440 ± 40	22 ± 1	11 ± 2